

Report to the XIII International Conference on
High Energy Physics, Berkeley (1966)

ELECTRODYNAMIC INTERACTIONS*

S. D. Drell

Stanford Linear Accelerator Center
Stanford University, Stanford, California

*Work supported by the U. S. Atomic Energy Commission.

I have major experimental progress to report in three areas. These are 1) the electromagnetic form factors of the proton at large space-like and time-like values of the square¹ of the invariant momentum transfer q^2 ; 2) the photoproduction of electron-positron and muon pairs as high momentum tests of quantum electrodynamics (Q E D); and 3) the muon $g-2$ value. Along with recent progress in other related experiments these new results have significant theoretical implications for our understanding of the hadron form factors and for increasing or delineating the domain of validity of Q E D. I will discuss these implications also in this report.

I. Hadron Form Factors

In three separate contributions from three experimental groups at DESY elastic electron proton scattering has been measured up to a momentum transfer of $q^2 = 10 \text{ (GeV/c)}^2$. Two of the experiments were performed with an internal liquid hydrogen target and one with an extracted electron beam incident on an external target. In the first internal target experiment² measurements were performed over a momentum transfer range from 0.6 (GeV/c)^2 to 4 (GeV/c)^2 by momentum analyzing the scattered electrons in either of two quadrupole spectrometers that, between them, covered the angular range of 32° to 130° . Absolute cross section calibrations were obtained by making measurements at $q^2 = 0.4 \text{ (GeV/c)}^2$ by directly detecting the recoil protons and normalizing the results of these additional measurements to the Rosenbluth formula using earlier Stanford work³ at lower energies but the same q^2 which yielded form factors to a $\pm 1.5\%$ precision.

In the second experiment⁴ the measurements were extended to large values of q^2 up to 10 (GeV/c)^2 using about 100 multitraversals of the 11 mm. diameter hydrogen target. The technique here was the "beam-bump" method of bringing the electron beam onto the target by turning on an additional magnetic field at the end of the acceleration cycle and then letting the beam circulate stably for a long time. This enabled cross sections as small as $5 \times 10^{-38} \text{ cm}^2/\text{ster}$ to be measured at a counting rate of 3 events per hour. Although quantameter measurements were used here as in the first experiment for beam monitoring, an absolute cross section calibration was achieved by periodically repeating the low q^2 measurements where, as remarked earlier, prior Stanford work³ provided accurate form factors for the calculation of the proton cross section. An accuracy in cross section of 10% was achieved up to $q^2 = 8 \text{ (GeV/c)}^2$ and of about 40% at 10 (GeV/c)^2 . At these large q^2 values the scattering angle was also large and measurement of the cross section yields the magnetic form factor, G_M , directly since the contribution of the electric term, G_E , is \lesssim a few percent.

In both of these internal beam experiments it is necessary to assume validity of the Rosenbluth straight line

$$F(E, \theta) \left(\frac{d\sigma}{d\Omega} \right)_{\text{lab}} = a (q^2) + b (q^2) \cot^2 \frac{\theta}{2} \quad (1)$$

(E is the incident electron energy and θ the scattering angle of the electron in the lab system; F is a known kinematic function) up to higher energies than had been tested. This was checked by measuring the small angle cross sections of $q^2 = 0.5 \text{ (GeV/c)}^2$ using the quantameter as an absolute monitor. The beam intensity was turned down so that the quantameter constant, as determined by a Faraday cup, could be used; 10% corrections were made for bremsstrahlung in the target cup.

To within experimental errors no deviations were found from the Rosenbluth straight line extrapolation.

Finally a third experiment⁵ utilized an external electron beam to make small angle scattering measurements out to 25° and $q^2 = 4 \text{ (GeV/c)}^2$ with a precision of typically $\pm 3\%$. Once again identification and analysis of the elastically scattered electron was achieved by means of a magnetic spectrometer system. In this case absolute normalization of the cross section was accomplished by direct monitoring of the external beam intensity with a Faraday cup. These measurements combined with the internal beam experiments at DESY plus earlier Stanford,³ CEA, Cornell, and Orsay work⁶ allowed separation of the charge and magnetic form factors up to 3 (GeV/c)^2 .

The results of all these experiments can be summarized as follows: The Rosenbluth straight line, Eq. (1), continues to describe the data very well up to $q^2 \approx 1.5 \text{ (GeV/c)}^2$ as shown for example in Fig. 1 and no deviations appear up to $q^2 \approx 3 \text{ (GeV/c)}^2$ although the accuracy here is less significant. This test of the analysis of electron-proton scattering is consistent with the interpretation of the data in terms of form factors and these are shown in Fig. 2. They satisfy the following three general features:

- 1) Within experimental errors the proton form factors are proportional to each other up to $q^2 = 3 \text{ (GeV/c)}^2$:

$$G_{Ep}(q^2) = G_{Mp}(q^2)/\mu_p \quad (\equiv 1 \text{ at } q^2 = 0) \quad (2)$$

- 2) A simple dipole distribution in momentum space provides a one parameter representation of all data

$$G_{Ep}(q^2) = \frac{G_{Mp}}{\mu_p} = \left\{ \frac{1}{1 + q^2/0.7 \text{ (GeV/c)}^2} \right\}^2 \equiv G(q^2) \quad (3)$$

- 3) There is no suggestion of a hard core, i.e., the form factors tend to zero for large q^2 .

In comparison with the CEA data⁶ of 1965 the form factors are smaller by as much as a factor of 1.7 at the highest q^2 values. Although this difficulty awaits experimental resolution the theoretical light we have shed on this subject is invariant under such small perturbations--a remark I am not proud to make.

There are two other new experimental results relevant to the validity of the Rosenbluth formula and the form factor interpretation of the data based on the assumption that one photon exchange between the electron and proton is an accurate approximation of the total interaction mechanism:

- 1) The ratio of positron-proton to electron-proton scattering measures the real part of the interference between first and second Born terms as illustrated in Fig. 3. Although the two photon exchange amplitude is reduced by a power of the fine structure constant, the possibility of polarizing the proton and exciting intermediate resonances makes $\text{Re}(A_1 A_2^*)/|A_1|^2$ an important ratio to measure (in spite of the theoretical predictions⁷ that the resonance excitations enhance the imaginary part of the two photon exchange amplitude which is $\frac{\pi}{2}$ out of phase and therefore does not interfere with the first Born amplitude). Fig. 4 shows the recent Cornell⁸ and CEA⁹ data on this ratio, $R = \frac{\sigma(e^+p)}{\sigma(e^-p)}$, up to $1.4 (\text{GeV}/c)^2$ together with the earlier Stanford data.¹⁰ Radiative corrections to this ratio are less than 2% at the largest q^2 and have been included. In both experiments the e^\pm beam was produced by converting the bremsstrahlung from the internal electron beam and the elastic scattering event was identified by detecting the scattered positron or

electron and the recoil proton in coincidence. Both experiments use spark chambers for precise angular measurements to reject inelastic events. The Cornell group used Cerenkov shower counters to identify the scattered electron and measure its energy; the CEA experiment had a thick plate spark chamber for electron identification. One has to judge for himself whether or not significant deviations from the Rosenbluth formula are indicated.

In proceeding with a theoretical interpretation we shall continue to assume validity of the one photon exchange formula. It is of some interest to comment that deviations of the ratio R from unity can be a very much more sensitive probe of corrections to the Rosenbluth formula than is observation of a deviation from a straight line as in Eq. (1). For example the amplitude describing the exchange of an axial meson (i.e., a dominant momentum transfer channel with unit spin and even charge conjugation) between the electron and proton will alter the ratio R since it does not flip the electron helicity and therefore it interferes with the one photon exchange amplitude in the relativistic limit of a massless electron. If the coupling of this channel is specified so that $R = 1.1$ at $q^2 \sim 0.8$ (GeV/c)² it would still require¹¹ experiments with a precision of better than 1% up to at least 20 GeV in order to detect a deviation from linearity in Eq. (1).

2) Also reported was a new observation of the polarization of the recoil proton which measures the imaginary part of the two photon exchange amplitude. At $E = 900$ MeV and $q^2 \sim 0.4$ (GeV/c)² the polarization of the proton in the direction normal to the electron scattering plane was measured¹² to be

$$P = (1.3 \pm 2)\%$$

For comparison we quote the earlier Orsay result¹³ of

$$P = (4 \pm 2.7)\%$$

at $E = 950$ MeV and $q^2 \sim 0.6$ (GeV/c)². In the first Born approximation of one photon exchange $P = 0$.

What do we make of these results theoretically? The only very simple theory would be based on a resonance model describing the exchange of one or of a few of the identified neutral vector mesons (or resonances) to the proton line as in Fig. 5. In the dispersion integral for the form factor

$$G(q^2) = \int_0^{\infty} \frac{\rho(\sigma^2) d\sigma^2}{\sigma^2 + q^2} \quad (4)$$

each of these will contribute a bump to the spectral amplitude $\rho(\sigma^2)$ at the mass of the exchanged resonance $\sigma^2 = M_r^2$. For large positive values of q^2 corresponding to high momentum transfer elastic scattering we can neglect the relatively narrow width of the resonances and write

$$G(q^2) \cong \sum_{\text{resonances}} \frac{A_r}{q^2 + M_r^2} \quad (5)$$

To fit the dipole distribution (Eq. 3) which falls for large q as q^{-4} requires the condition

$$\int \rho(\sigma^2) d\sigma^2 \cong \sum_r A_r = 0 \quad (6)$$

and to reproduce the measured proton charge and magnetic radius requires

$$6 \int \frac{\rho(\sigma^2) d\sigma^2}{\sigma^4} \cong \frac{6 \sum_r A_r / M_r^4}{\sum_r A_r / M_r^2} = (0.816 f)^2 \quad (7)$$

A fit to the data on this basis in terms of known resonances has not been achieved¹⁴ and the search for plausible reasons has been active and diverse. Three routes presented to the conference have been:

1) Multiply the expression in Eq. (5) $G(q^2)$ by a form factor $f(q^2)$ for the vector meson-nucleon (or electromagnetic current) coupling.¹⁵ A one parameter fit is possible with

$$f(q^2) \approx \frac{1}{1 + q^2/(\text{GeV}/c)^2} \quad (8)$$

2) Couple the vector mesons to the individual quarks in the proton and multiply $G(q^2)$ in Eq. (5) by a distribution function $W(q^2)$ representing the fourier transform of the wave function for the quark motion¹⁶ about the center of mass of the proton. Again a one parameter fit can be constructed as in Eq. (8) the only difference being the interpretation of $W(q^2)$ in place of $f(q^2)$.

3) Turn to an infinite component field theory¹⁷ such as grow out of attempts to construct a relativistic generalization of SU(6). One such example is SL(6,C), the group of unimodular 6 x 6 matrices. The local field operator in this theory is an infinite tower producing an infinite number of baryon states of the same mass. In such theories the operator projecting a proton out of this infinite tower introduces kinematic or momentum dependent factors that serve to reduce the amplitude of the proton's transition charge density, i.e., the matrix elements in momentum space of scalar products of the field operators for initial and final protons of different momenta, p and $p + q$ respectively. This occurs because an initial proton overlaps more and more with the

the higher baryons when given larger and larger momentum transfers and so more of the transition amplitude is lost from its projection onto the final recoiling proton state. The additional multiplying factor in this theory takes the form of $\left[\frac{1}{1 + q^2/4M_p^2} \right]^{7/2}$ for an SL (6,C) scalar matrix element. This kinematical factor is assumed to multiply the simple vector pole describing the dynamics in the local field theory constructed for the infinite local field tower.

In such a theoretical description there still remains a broad divergence of theoretical opinions¹⁸ as to whether or not it is possible to harmonize the requirements of locality, statistics, and the assignment of the nucleon to the 56 representation. Unfortunately I am not competent to predict whether or not the SL (6,C) theory will survive these major challenges, just as I am unable to resolve the disagreements between different experiments on electron proton scattering and in the other measurements I still want to discuss in my report! Fig. 6 shows the success of the dipole fit to the form factors, as well as the apparently too rapid fall off of SL (6,C) predictions for large q^2 . In drawing the SL (6,C) curve for G_M I have made the arbitrary assumption that the scalar matrix element applies to the magnetic form factor as well as the electric one. An alternate possibility is to assign the transformation properties of the tensor operator that generates the 70 in SL (6,C) to the current vector,¹⁹ but then an even more rapid decrease with large q^2 is suggested.

A fourth possibility for interpreting the $G(q^2)$ behavior summarized in Eqs. (6), (7), and (8) was not presented to this conference and is to be classified as part of the folklore but is not to be dismissed

on experimental grounds alone. It is that the observed G is the product of Yukawa form factors representing electron as well as proton size. We can write in reasonable agreement with the electron proton scattering data

$$G(q^2) = \left\{ \frac{1}{1 + q^2/M_p^2} \right\} \left\{ \frac{1}{1 + q^2/1.1 (\text{GeV}/c)^2} \right\}$$

where the first factor represents the proton structure corresponding to ρ^0 exchange and the second one represents a possible electron size with the indicated cut-off mass within the one standard deviation limit derived from the published e-e colliding beam measurements.²⁰

If we confine our attention to the asymptotic behavior of $G(q^2)$ for large q^2 we may turn to a suggestion by Wu and Yang²¹ of two years ago that the electromagnetic form factor should decrease exponentially with the momentum transfer as the one-fourth root of the p-p differential cross section, i.e.,

$$G(q^2) = e^{-q/(0.6 \text{ GeV}/c)} \quad q > 1 \text{ GeV}/c \quad (9)$$

This model provides a no parameter fit to the slope of $G(q^2)$ and is based on the very simple physical notion that the proton, like a fragile bowl made of glass or china, shatters identically into many pieces when hard hit, no matter what the projectile. A fit of this model of the DESY data is shown in Fig. 7 and does very well. Clearly more data on $G(q^2)$ is needed to tell the story, but already there is one lesson here for all who parametrize the form factors--we still cannot really distinguish between exponential and power fall off with the data at hand!!

It has just become possible to draw this distinction for the deuteron form factor as derived from accurate data on elastic electron-deuteron scattering. Recent experiments²² at CEA extend over a sufficiently broad range with high accuracy to exclude a simple exponential fit of the Wu-Yang type for the deuteron in favor of one with a positive curvature on a logarithmic scale as shown in Fig. 8. A fit to this data is possible with a fractional experimental form $e^{-(q/q_0)^x}$ with $x < 1$ and more detailed analysis is now in progress. An analogous fit to the large q behavior of the proton form factor is also possible within the broad limits still permitted by present data and Fig. 9, for example, shows a fit to the proton form factors of a square root exponential. The modulated curves shown by dotted lines in Fig. 9 are derived theoretically²³ for a system of one charged and one electrically neutral particle bound with a $\frac{1}{r^4}$ repulsive core static potential in a nonrelativistic Schrodinger description. They are intended only to illustrate the possibilities of this class of asymptotic fits. Several comments are of interest with regard to these large q fits:

a) The exponential form of Eq. (9) has the attractive feature of being the most rapidly decreasing form factor consistent with polynomial boundedness.²⁴ In other words a more rapid decrease would deny us the possibility of writing dispersion relations for form factors (and hence must not be tolerated!). Thus we have a minimal principle that e^{-q/q_0} is the most rapidly decreasing form factor allowed by dispersion theory.

b) A repulsive core potential introduces an essential singularity in the wave function of a bound system for zero particle separation and cannot lead to an exponential fall off in q but only to a modulated

fractional exponential law²³ of the form

$$G(q^2) \Rightarrow e^{-(q/q_0)^{p/p+1}} \sin \left\{ (q/q_0)^{p/p+1} + \phi_p \right\} \text{ for } q/q_0 \gg 1 \quad (10)$$

where p is defined by the power, $\frac{1}{r^{2(1+p)}}$ of the repulsive potential, and ϕ_p is a phase.²⁵

c). The observations in (a) and (b) are made modulo the multiplication of $G(q^2)$ by a finite positive or negative power of q . The parameters in the dotted curve of Fig. 8 correspond to a radial solution behaving for $r \rightarrow 0$ as $e^{-a/r}$ for a $1/r^4$ potential and are altered if solutions of the form $r^m e^{-a/r}$ are specified. Once we are in the asymptotic region these powers should not play a crucial role and this region of asymptotically large q can be ascertained by plotting the function

$$\frac{\ln [G(q^2)/\sin \left\{ (q/q_0)^x + \phi_x \right\}]}{(q/q_0)^x}$$

and seeing if it can be made to approach a horizontal asymptote for some positive value of x .

d) In applying these model considerations to the proton we have in mind a three-massive-quark model. The same form as Eq. (10) can be derived in this case²³ as for the two particle deuteron.

e) The more rapid the rate of decrease of G for large space like q^2 , the more stringent are the restrictions on the absorptive amplitude $\rho(\sigma^2)$ in Eq. (4). In particular if G decreases faster than any power of q , ρ and therefore the imaginary part of G must oscillate an infinite number of times for time-like values of $|q^2|$ as occur in the annihilation process

$$e + \bar{e} \leftrightarrow p + \bar{p} .$$

This does not mean that the magnitude of G which is the experimentally measured quantity need oscillate; par. ex. $|e^{iq}| = 1$.

Such a behavior in any case is not inconsistent with the meager data available thus far on the annihilation cross section of $p + \bar{p}$ to lepton pairs but further data will be of great significance in this regard.

For $|q^2| = 6.8 \text{ (GeV/c)}^2$ the Cal Tech-Brookhaven group reported an upper limit (90% confidence) to the $p\bar{p}$ annihilation cross section to $e\bar{e}$ at 90° of $\leq 4 \times 10^{-35} \text{ cm}^2/\text{ster}$ compared to the earlier CERN limit²⁶ of $\leq 10 \times 10^{-35} \text{ cm}^2/\text{ster}$ to $e\bar{e}$ and $\leq 5 \times 10^{-35} \text{ cm}^2/\text{ster}$ to $\mu\bar{\mu}$. In terms of a form factor this means that $G_M/\mu \lesssim 0.04$ (combining experiments) compared with the value of $G_M/\mu = 0.008$ reported by DESY (see Fig. 2) for the corresponding space-like momentum transfer in the electron-proton scattering. Another way of representing the significance of this number is illustrated in Fig. 10. The 90% confidence limit shown there is obtained by combining the CERN and Brookhaven experiments and lies above the theoretical curve for a normalized form factor G based on a dipole distribution, Eq. (3), for time-like as well as space-like values of q^2 . In fact $G(q^2)$ will approach the same limit for large space-like and time-like values of $|q^2| > 4 M_p^2$, as occur in the scattering $e + p \rightarrow e + p$ and annihilation $p + \bar{p} \leftrightarrow e + \bar{e}$, respectively, whenever the dominant contributions to the spectral amplitude in Eq. (4) come from states such as the ρ^0 , ω , and ϕ of low masses. This is an example of the Phragmen-Lindelof theorem.²⁷ The exponential forms discussed in Eqs. (9) and (10) arise because there are important contributions to the spectral amplitude $\rho(\sigma^2)$ from states of all masses and these lead to an infinite number of oscillations in ρ . These are examples of the class of functions escaping the Phragmen-Lindelof restriction.

In view of the massive efforts at both CERN and Brookhaven to establish even these rather liberal upper limits on the proton form factors

via the annihilation process

$$\begin{aligned} p + \bar{p} &\rightarrow e + \bar{e} \\ &\rightarrow \mu + \bar{\mu} \end{aligned}$$

it is highly unlikely that further experimental information $G(q^2)$ for time like q^2 will be forthcoming until high luminosity colliding electron-positron rings of sufficient energy are constructed.

In concluding our form factors discussion we note briefly several other new results on neutron and pion structure:

1) New measurements on the ratio of the electron-neutron to the electron-proton elastic scattering cross sections were reported²⁸ from CEA in the range of $q^2 = 0.27$ to 4.5 $(\text{GeV}/c)^2$. These were made using the external electron beam at CEA and measuring electron, proton coincidences from deuterium. An event in which the scattered electron is observed with no coincidence is attributed to electron-neutron scattering. Above $q^2 = 1.16$ $(\text{GeV}/c)^2$ the observations are consistent with the scaling law

$$G_{Ep} = \frac{G_{Mp}}{\mu_p} = \frac{G_{Mn}}{\mu_n} \quad \text{and} \quad G_{En} = 0 \quad (11)$$

as shown in Fig. (11). At lower values of q^2 a proportionality relation Eq. (11) remains valid for the magnetic form factors but now the neutron's Dirac form factor $F_{1n} = 0$, a result which joins smoothly to the vanishing slope of F_{1n} for $q^2 \rightarrow 0$ as found from electron-neutron interaction experiments at zero energy.²⁹

2) The charge radius of the charged pion is also being measured. High precision has not yet been achieved in this program and all that can be said is that the evidence favors a pion form factor not very

different from that of the proton, which is as it should be on the basis of a ρ -dominant exchange model between the electromagnetic current and the pion line. At Cornell the program of measurements is being pursued via the electropion production process in hydrogen³⁰ with the kinematic variables adjusted to maximize the exchange pion pole, illustrated in Fig. 12, and with the kinematics varied to permit separation of the longitudinal and transverse matrix elements. In this way sensitivity to the theoretical models can be probed. The eventual accuracy that can be achieved this way is not completely clear in view of the limitations in accuracy of theories of pion photoproduction by real as well as by virtual photons.

Direct pion charge radius measurements are also being attempted³¹ by analysis of $\pi^- - e^-$ scattering as well as by detailed theoretical and experimental study of the difference in $\pi^+\alpha$ and $\pi^-\alpha$ cross sections.

II. Photoproduction of Large Angle Pairs

Let us turn next to large angle pairs and the status of Q E D for electrons and muons. In symmetric pair experiments there is a large momentum transfer to the leptons that are photoproduced at wide angles ($\theta_e \gg m_e/k$) and a low momentum transfer to the target proton or nucleus. The role of the nucleus in these processes can be summarized in terms of measurable form factors from elastic and inelastic scattering, without introducing unknown strong interaction dynamics, to lowest order in $Z\alpha$. It is thus possible to probe quantum electrodynamics for the virtual electron or muon line in Fig. 13a propagating far from its mass shell.³² Background contributions arise from virtual compton amplitudes as illustrated in Fig. 13b. In a symmetric arrangement, however,

interference between the Bethe-Heitler and Compton terms vanishes since the Bethe-Heitler cross section is invariant under the interchange of e and \bar{e} (or μ and $\bar{\mu}$) in this case whereas the interference term is odd. The square of the virtual compton amplitude can be dismissed as completely negligible except for photoproducing lepton pairs at the masses of the vector resonances³³ (ρ^0 , ω , ϕ).

The initial CEA measurements³⁴ of electron pair production were in gross disagreement with theory and either they had to change, or new theoretical corrections found, or Q E D was in trouble. Predictably, greatly heightened interest in this process was aroused by those results. The CEA measurements were made for electron momenta from 0.5 to 2.5 GeV/c and from pair angles of $\theta = 4.6$ to 7.5° , spanning the range of invariant masses of the pairs up to $Q_M \approx 600$ MeV.

The general technique in such an experiment is to look at the electron pairs from a carbon target with two mirror image spectrometer systems. The CEA experiment determined particle momenta with quadrupole spectrometers and discriminated against very high pion backgrounds with a combination of threshold Cerenkov and shower counters. At Cornell³⁵ a similar experiment was performed at somewhat lower energies and masses and using spark chambers for particle identification: thin plate chambers for observing trajectories through a bending magnet and thick plate chambers to identify electrons by their shower producing properties. After all corrections due to hard photon radiative corrections and due to the finite target thickness degrading the energy of the emerging electrons were included, both the CEA and Cornell experiments as reported to this conference normalized correctly to the Bethe-Heitler cross section at low momenta. However the experimental points exceeded the

very rapidly falling [$\propto 1/k^3 \theta^6 \propto k^3/Q_M^6$] theoretical predictions for large Q_M by a factor of more than two at the highest Q_M values. Such a result is quite a jolt to us!

From a Columbia-DESY collaboration³⁶ we now have a new report of another symmetric electron pair experiment covering the same kinematic range as the CEA experiment. Electrons produced in the carbon target were first bent away from the beam by a large bending magnet and then bent back toward the beam line by two more bending magnets. The electrons were separated from other particles by two gas threshold counters and a shower counter for both the e^+ and e^- arms; these six counters gave an overkill of the background particles (predominantly pions) which was verified by comparing counting rates obtained when various of these counters were taken out of coincidence. Continuous checks were made, including checks on the dead time corrections of the coincidence circuits and on the operation of the quantameter which was monitored with a counter telescope viewing a copper plate in the beam. A complete analysis of all radiative corrections to the data has yet to be completed but remaining corrections are thought to be energy independent and of the order of 5%. In Fig. 14 all data of the three experiments are shown but without inclusion of the full radiative corrections to the DESY-Columbia data as remarked above. No disagreement is found between DESY-Columbia and theory but a real discrepancy with the earlier experiments remains to be understood and resolved.

In the analogous experiment on the photoproduction of symmetric mu-pairs the trend of the data is presented as being away from agreement with theory. This is a CEA experiment³⁷ and each detected muon was in the energy interval of 1.8 to 2.4 GeV and in an angular range extending

from $\theta = 4.2^\circ$ to 10.9° . Restricting the discussion to high energy points such that the individual muon energies exceed 2.04 GeV in order to reduce the severity of π pair backgrounds, we show in Fig. 15 the ratio R of experiment to Bethe-Heitler theory. The experimental errors as shown are dominated almost entirely by systematic errors. The fact that the ratio does not properly normalize to unity is believed to be due to systematic factors that are energy independent.

If we accept as a real effect the negative slope of R in Fig. 15 which was computed to be a $2\frac{1}{2}$ standard deviation disagreement with a horizontal line, then we must challenge Q E D. Once we are producing pairs with a total mass equal to that of the ρ^0 then the excess in experiment above Bethe-Heitler pair production coupled with known data in ρ^0 photoproduction cross sections gives a measure of the $\rho^0 \rightarrow \mu^+ + \mu^-$ partial decay rate. However, since there is no interference between the Bethe-Heitler and the virtual Compton process there can be no dip below a unit ratio.³⁸

Further experimental analysis should settle these challenges to Q E D before long. In the meantime this experiment on μ pair production at the ρ^0 mass can be combined with others recently performed to put limits on the decay branching ratios of neutral vector mesons to lepton pairs. The numbers in the following table are consistent with simple theoretical models but as yet do not offer crucial tests or checks.

BRANCHING RATIOS FOR DECAY OF VECTOR MESONS
TO LEPTON PAIRS

dePagter, et. al., P.R.L. 16, 35 (1966)

$$\frac{\rho \rightarrow \mu^+ + \mu^-}{\rho \rightarrow \text{all}} = 0.44 \begin{matrix} +0.16 \\ -0.07 \end{matrix} \times 10^{-4}$$

Zdanis, et. al., P.R.L. 14, 721 (1965)

$$\frac{\rho \rightarrow e^+ + e^-}{\rho \rightarrow 2\pi} = 0.5 \begin{matrix} +0.6 \\ -0.3 \end{matrix} \times 10^{-4}$$

$$\frac{\omega \rightarrow e^+ + e^-}{\omega \rightarrow 3\pi} = 1.0 \begin{matrix} +1.2 \\ -0.8 \end{matrix} \times 10^{-4}$$

Binnie, et. al., P.L. 18, 348 (1965)

$$5 \times 10^{-5} < \frac{\omega \rightarrow e^+ + e^-}{\omega \rightarrow 3\pi} < 60 \times 10^{-5}$$

III. g-2 Value of the Muon

Finally I want to turn to the new results on the muon g-2 value and to a review of some of the successes and strains facing Q E D in the low-energy precision realm. CERN has brought into operation a muon storage ring³⁹ into which an external proton beam of 10 GeV energy impinges producing pions in a target. Negative pions of momentum 1.3 GeV/c are trapped and in the first turn around the ring of 5 meters diameter 20% of the pions decay. The decay muons at small forward angles will have the proper momentum ≈ 1.2 GeV/c to be trapped and circulate in the ring while at the same time being highly polarized (97% on the average). Since they are highly relativistic ($\gamma \sim 12$), their mean lifetime is dilated to 27 μ sec. On the other hand the precession period of their spin relative to their momentum vector is the same as for the nonrelativistic muon. This allows the precession to be followed to more

than 20 precession cycles as illustrated by the data in Fig. 16. In the original low energy CERN μ^+ experiment⁴⁰ typically one precession cycle was followed. Accurate determination of the magnetic field strength, as required, is achieved in this experiment by making accurate measurements of the radius of orbit of muons in the ring by measuring their rotation frequency during their first few rotations. Analysis of the μ^- precession is made by observing the decay in flight of muons in the ring magnet. Only the forward decaying electrons are observed by means of a total-absorption lead-scintillator sandwich counter.

The CERN report to the conference recorded successful μ^- storage in the initial tests and with one counter and only 5 hours of operation has already bettered the accuracy of the earlier measurement on the g-2 value of the μ^+ by a factor of two. The comparison with theory⁴¹ is as follows:

$$\begin{aligned}
 A_{th} &= \left(\frac{g-2}{2} \right)_{theory} = \frac{\alpha}{2\pi} + 0.766 (\alpha/\pi)^2 \\
 &= 1165 \times 10^{-6}
 \end{aligned}
 \tag{12}$$

Old μ_+ :

$$\begin{aligned}
 A_+ &= (1162 \pm 5) \times 10^{-6} \\
 &= A_{th} - (\frac{1}{2} \pm 1) (\alpha/\pi)^2
 \end{aligned}$$

New μ_- :

$$\begin{aligned}
 A_- &= (1165 \pm 3) \times 10^{-6} \\
 &= A_{th} \pm 0.6 (\alpha/\pi)^2 \\
 &= A_{th} \pm 250 (\alpha/\pi)^3
 \end{aligned}$$

The excellent agreement of μ^+ and μ^- g values to 6 ppm is the most precise confirmation of TCP as symmetry operation for muon interactions.³⁹

While saluting this achievement we cannot refrain from wondering what will be found if another factor of 30 in accuracy can be achieved and $\frac{g-2}{2}$ is determined to one part in 10^7 , i.e.,

$$\Delta \left(\frac{g-2}{2} \right) \approx 10^{-7} \approx 8 (\alpha/\pi)^3. \quad (13)$$

This is still an order of magnitude above the uncertainty introduced by our present imperfect knowledge⁴² of α :

$$\delta (\alpha/2\pi) \approx \pm 0.4 (\alpha/\pi)^3 \quad (14)$$

but is comparable with anticipated contributions to $g-2$ arising from the contributions of strongly interacting particles,⁴³ the ρ^0 in particular, to the photon vacuum polarization as illustrated in Fig. 17. On the basis of a ρ dominant model in the iso-vector channel of ep scattering we expect a contribution of order of magnitude

$$\Delta \left(\frac{g-2}{2} \right) \approx \frac{\alpha^2}{3\pi} (m_\mu/M_\rho)^2 \approx 8 (\alpha/\pi)^3$$

This result is comparable to estimates of the weak interaction contributions⁴⁴ if the W meson exists. No matter how heavy the W may be, if it exists and gives rise to a first order contribution to $(g-2)$ in the weak coupling strength as illustrated by Fig. 18 we anticipate contributions⁴⁵ to $\frac{g-2}{2}$ of $\approx 3 (\alpha/\pi)^3$ (magnetic and quadrupole moments of the W could increase this considerably).

There will also be sixth order purely electromagnetic contributions enhanced by the logarithm or the square of the logarithm of the muon-electron mass ratio, i.e., of order

$$\left(\frac{\alpha}{\pi}\right)^3 \ln^2(m_\mu/m_e)^2 \quad \text{and} \quad \left(\frac{\alpha}{\pi}\right)^3 \ln(m_\mu/m_e)^2.$$

These arise from electron vacuum polarization bubbles inserted into second and fourth order contributions that have already been computed. They contribute to the moment of the muon⁴⁶

$$\Delta\left(\frac{g-2}{2}\right)_{\text{pol}} = \frac{\alpha}{2\pi} \left(\frac{\alpha}{3\pi}\right)^2 [\ln^2(m_\mu/m_e)^2 - 10.02 \ln(m_\mu/m_e)^2 + 0(1)] \quad (15)$$

$$< (\alpha/\pi)^3$$

The possibility that the scattering of light-by-light insertion gives rise to logarithmically enhanced sixth order contributions is still not resolved but will also have to be included in addition to Eq. (15) if results to an accuracy indicated in Eq. (13) are to be interpreted.

We have before us then the very exciting prospect of observing in an isolated electrodynamic system, deviations from a purely Q E D behavior due to coupling with the world of strong and weak interaction physics. In this aspect the muon g-2 value is more exciting than that of the electron for which the contributions of these interactions are scaled down by the square of the electron to muon mass ratio.

Lest this report lead one to conclude all is well once again with Q E D let me close with a few observations on the hyperfine splitting of the ground state of the hydrogen atom and on the Lamb shift in hydrogen.

The hyperfine splitting (hfs) in atomic hydrogen is an important link between the usually disjoint fields of high energy and precision atomic physics. This is because the hfs is sensitive to details of the proton structure which are usually seen only in high energy electron-proton elastic and inelastic scattering experiments. The possibility that there exists a discrepancy between very accurate experimental measurements and theoretical calculations has stimulated a lot of recent work on this subject and the way things stand at the moment is as follows.

In comparing the very precise experimental number on the triplet-singlet splitting in the hydrogen atom ground state⁴⁷

$$\nu_{\text{expt}} = (1420.40571800 \pm 28 \times 10^{-9}) \text{ MHz.} \quad (16)$$

with the theoretical formula,⁴⁸ the greatest error is introduced by the uncertain value of the fine structure constant,⁴² α , in Eq. (14) and by the uncertain magnitude of the proton structure corrections. The most accurate value of α has been determined from the measurement of the fine structure interval in the deuterium atom--i.e., the energy interval between the $2p_{3/2}$ and $2p_{1/2}$ levels and is⁴⁹

$$\alpha^{-1} = 137.0388 (1 \pm 9 \text{ ppm}) \quad (17)$$

The quoted error is larger than the two standard deviations figure and represents the limit of error. In the theoretical calculation of ν all purely electrodynamic contributions are included to a precision of better than⁴⁸ 1 ppm. Moreover if the proton is treated as a rigid golfball or baseball its interaction can be completely summarized in terms of its charge and magnetic form factors as measured in the electron elastic

scattering experiments described at the beginning of this report.⁵⁰
On this basis we arrive at a comparison between theory and experiment
that can be expressed in the form⁵¹

$$\frac{\nu_{\text{rigid}}}{\nu_{\text{expt}}} = (137.0388\alpha)^2 [1 - (43 \pm 2) \times 10^{-6}] \quad (18)$$

In assessing whether or not Eq. (18) is to be interpreted as a
fundamental challenge to Q E D two questions come up:

- 1) On the theoretical side, it is clear that the rigid
baseball model of the proton is a gross oversimplification.
In fact the proton is a highly polarizable structure as
is evidenced by the large magnitude of the photo- and
electro-production cross sections of mesons from protons
as well as by the many resonances contributing. How big
are these proton polarizability contributions to ν ?
- 2) On the experimental side new measurements of the Lamb shift
in hydrogen, i.e., the splitting $2s_{1/2} - 2p_{1/2}$, by Robiscoe
and co-workers⁵² are significantly larger than the earlier
ones. How does this effect the total fine structure interval
and thereby the experimental value of α in Eq. (17)?

In response to the first question, earlier theoretical studies^{50,53}
taking into account only the 33 resonance of the pion proton system in a
dispersion analysis have indicated a polarizability contribution of
 $\lesssim 1$ ppm. A different conclusion was reported to this conference⁵⁴
and it was argued that hitherto uncalculated parts of the proton structure
corrections involving the detailed behavior of non-resonant channels of
the electropion production amplitude may very well contribute ≈ 10 ppm

toward removing the possible discrepancy suggested in Eq. (18).⁵⁵

Attempts to calculate these contributions with dispersion theory run into the very same difficulties as attempts to calculate the neutron-proton mass difference: it is necessary to know details of the strong interactions⁵⁶ and there is no one dominant resonant channel such as the 33 resonance to rely on. Therefore an accurate result is impossible, and getting even the right sign⁵⁷ is a significant achievement!

A non-relativistic model of the proton as a bound structure obeying the Schrödinger equation provides some physical insight although no quantitative results. Calculation of the hfs with such a model⁵⁴ shows the rigid baseball limit described above as emerging in the limit that the excited nucleon states lie sufficiently high above the ground state that $\bar{\Delta W} \bar{R} \gg 1$ where $\bar{\Delta W}$ denotes an average excitation energy and \bar{R} the proton radius. In the opposite limit of $\bar{\Delta W} \bar{R} \ll 1$ the proton is highly polarizable. The orbital electron in the hydrogen atom and the proton mutually polarize each other so that the electron orbit is recentered about the instantaneous proton charge position as a result of their mutual coulomb attraction. This Born-Oppenheimer approximation applies when the proton excitation frequencies are small compared with the frequency of circulation of the near part of the electron amplitude at the proton surface, i.e., (in units of $c = 1$)

$$\frac{1}{\bar{R}} \gg \bar{\Delta W} \quad \text{or} \quad \bar{\Delta W} \bar{R} \ll 1.$$

In this case the electron can adjust its wave function to circulate around the instantaneous charge-current distribution so that the proton appears to be a point charge. The deuteron is a very loosely bound system and

the above criterion is well satisfied in the analysis of the deuterium hfs as first shown by A. Bohr.⁵⁸

Now the proton is less polarizable than the deuteron, its excited states lying at least 140 MeV above the ground state. Nevertheless there are important excitations with $\Delta\bar{W} \bar{R} \sim 1$ so that in part, at least, the electron can follow the instantaneous charge distribution in the proton. This will increase the calculated hfs-- and diminish the possible discrepancy in Eq. (18)--since the proton charge-current distribution will be seen by the electron to be more like a point than in its rigid baseball limit. On the basis of calculations with non-relativistic models this polarizability correction was found to be sizable.

In response to the second question on the value of α all that we can say at the moment is that resolution of an experimental disagreement is needed. The total fine structure interval $2p_{3/2} - 2p_{1/2}$ is more than 10 times as large as the Lamb shift interval $2s_{1/2} - 2p_{1/2}$. It is measured by adding the transition frequencies $(2p_{3/2} - 2s_{1/2}) + (2s_{1/2} - 2p_{1/2})$ and from this the value of α is obtained as quoted in Eq. (17). It has not been remeasured. What has happened is that a new measurement⁵² of the Lamb shift interval is larger by ~ 0.3 MHz than the previous results. If this increase is simply, and without further justification, added on to the total fine structure interval the value of α increases by 13.5 ppm and Eq. (18) can be written more comfortably as

$$\frac{\nu'_{\text{rigid}}}{\nu_{\text{expt}}} = 1 - (16 \pm 20) \times 10^{-6} \quad (19)$$

where the uncertainty of $\pm 20 \times 10^{-6}$ is no more than the sum of ± 14 ppm

for the error in α as in Eq. (17) and of ± 2 ppm which is the theoretical estimate of the uncertainty introduced by the form factors.⁵¹ Eq. (19) if true suggests no serious problems for the hfs no matter whether the polarizability contributions are ultimately confirmed as being $\lesssim 1$ ppm or ~ 10 ppm.

One can turn to the muonium ($\mu^+ - e^-$) atom for a precise analysis and data on the hfs that is free of the uncertain polarizability correction due to proton dynamics. Although an increase in α by 13.5 ppm will disturb the existing close agreement of theory and experiment,⁵⁹ Ruderman⁶⁰ has pointed out that a chemical shift correction has been overlooked in the determination of the absolute magnitude of the muon magnetic moment. The ratio of the magnetic moment of a μ^+ meson to that of the proton is determined by measuring the ratio of their precession frequencies in a magnetic field for μ^+ mesons stopped in water (and aqueous HCl). However if the chemical environment of the μ^+ in water differs from that of the proton due to a diamagnetic shielding correction the ratio of precession frequencies must be corrected to allow for this before the ratio of magnetic moments can be inferred. Ruderman has estimated this chemical shift by noting that a muon can form a type of bond between water molecules that is stronger than the usual hydrogen bond because of its lighter mass and higher zero point energy. This bonding remains unbroken during the microsecond lifetime of the muon so that the μ^+ does not simply replace a proton. In fact he estimates that the muon in this state sees a chemical shift of 20 ppm less than that of the proton and thereby the muon moment is correspondingly decreased by ~ 20 ppm below the published values. Such a change would almost completely absorb the increase in α^2 suggested (but not established) by the new Lamb shift measurement.

However while we await further clarification on the hfs front, the newly published value of the Lamb shift in hydrogen itself is in serious disagreement with theory. The older value as obtained by directly inducing the radiofrequency transition is⁴⁹

$$S = 1057.77 \pm .10 \text{ MHz} \quad (20)$$

Two new measurements⁵² of the Lamb shift have been made by inducing a level crossing of two different hyperfine lines of the $2s_{1/2}$ and $2p_{1/2}$ levels in a magnetic field whose strength is measured by observing the nuclear magnetic resonance of protons in water. Correcting back to the splitting in a zero magnetic field by the Breit-Rabi formula, these give individually for the Lamb shift

$$S = \begin{array}{l} 1058.07 \pm .10 \text{ MHz} \\ 1058.05 \pm .10 \text{ MHz} \end{array} \quad (21)$$

The quoted errors in Eqs. (20) and (21) are approximately three standard deviations. The latest theoretical value for the Lamb shift in H is

$$S_{th} = 1057.50 \pm .11 \text{ MHz} \quad (22)$$

as obtained by adding the fourth order radiative correction recently completed by Soto⁶¹ to the analysis of Erickson and Yennie.⁶² In view of the liberal allowance of error made to both the experimental and theoretical numbers it would appear to be difficult to harmonize Eq. (21) and (22). The Lamb shift itself is proportional to α^3 Rydbergs and therefore an increase in α of no less than 100-200 ppm would be required to remove this discrepancy, short of modification or addenda to the

theoretical formula⁶³ or to the theory of the experiment itself.

However so large a change in α would completely disrupt the hfs as we saw earlier.

By now I have strayed very far from the usual energy domain of $\sim 10^{+10}$ ev for a high energy conference to $\sim 10^{-9}$ ev in discussing a missing few tenths of a MHz in the Lamb shift. In fact, both domains are important in probing the detailed behavior of Q E D at small distances. The high energy road of large momentum transfer experiments and the low energy road of atomic measurements with extreme precision are two complementary routes for making progress toward the same goal. Moreover there is no unique or theoretically compelling figure of comparison between experiments in these two domains as to which is probing Q E D to a smaller distance or a higher momentum transfer. Depending on a particular choice of the form of a possible ad hoc modification in Q E D one or another experiment can be made to appear the more sensitive probe. Simplicity and the maintenance of Lorentz invariance have been the principle criteria in writing various proposed forms for the modifications of Q E D and the cut off momenta entering these ad hoc forms have had no significance beyond serving as mnemonic devices for characterizing different experiments.

In addition to these two there are other criteria which we might not like to violate even if there is a breakdown of Q E D and these introduce further severe restraints or possible forms for modifying the theory. Among these are the spectral conditions and differential current conservation. In a contribution to this conference Kroll⁶⁴ has shown that the full content of the latter requirement poses very severe limitations on possible propagator modifications in the large

angle pair experiments discussed earlier in Part II. A modification of the propagator for a charge bearing line such as appear in the Feynman graphs in Fig. 13 must be accompanied by a vertex modification in accord with the Ward-Takahashi identity if differential current conservation $\partial_j^\mu(x)/\partial x^\mu = 0$ is not to be sacrificed.⁶⁵ In addition there are restrictions requiring the introduction of many-photon vertices that Kroll has analyzed. These restrictions lead to the conclusion that possible deviations from the Bethe-Heitler formula for pair production must be proportional to the fourth power of the momentum transfer and not to the square for small values of the momentum transfer as has usually been assumed in describing these experiments. At present there is no clear cut experimental evidence on this score as we have seen in Part II. It will be important to retain or even test this restriction in future parametrizations of the ratio of experimental results to theoretical predictions of Q E D.

In closing I want to thank Dr. Robert Diebold, of SLAC, my scientific secretary for this conference, who provided very valuable aid in my appreciation of the new experimental results discussed in this report as well as in the preparation of the report itself.

FOOTNOTES AND REFERENCES

1. Throughout this report we use the convention $q^2 \equiv -|\Delta E^2 - \Delta P^2| > 0$ in the space-like region of momentum transfers as occur in electron-proton elastic scattering and $q^2 < 0$ in the time-like region probed in annihilation processes.
2. H. J. Behrend, F. W. Brasse, J. Engler, H. Hultschig, S. Galster, G. Hartwig, H. Schopper, and E. Ganszuage, submitted to XIII International Conference on High Energy Physics, Berkeley (1966).
3. T. Janssens, R. Hofstadter, E. B. Hughes, and M. R. Yearian, Phys. Rev. 142, 922 (1966).
4. W. Albrecht, H. J. Behrend, F. W. Brasse, W. Flauger, H. Hultschig, and K. G. Steffen, submitted to XIII International Conference on High Energy Physics, Berkeley (1966).
5. W. Bartel, B. Dudelzak, H. Krehbiel, J. M. McElroy, U. Meyer-Berkhout, R. J. Morrison, H. Nguyen-Ngoc, W. Schmidt, and G. Weber, submitted to XIII International Conference on High Energy Physics, Berkeley (1966); and Phys. Rev. Letters 17, 608 (1966).
6. K. W. Chen, J. R. Dunning Jr., A. A. Cone, N. F. Ramsey, J. K. Walker, and Richard Wilson, Phys. Rev. 141, 1267 (1965).
K. Berkelman, M. Feldman, R. M. Littauer, G. Rouse, and R. R. Wilson, Phys. Rev. 130, 2061 (1963).
B. Dudelzak, A. Isakov, P. Lehmann, R. Tchapoutian, Proc. of the XII Intern. Conference on High Energy Physics at Dubna 1, 916 (1964).
7. c.f. lectures on "Form Factors of Elementary Particles" in the Proceedings of the International School of Physics Enrico Fermi Course XXVI, p. 205-208 (Academic Press, 1963).
8. R. L. Anderson, B. Borgia, G. L. Cassiday, J. W. DeWire, A. S. Ito, and E. C. Loh, Phys. Rev. Letters 17, 407 (1966).

9. A. de Hollan, E. Engels, B. Knapp, and L. Hand, submitted to XIII International Conference on High Energy Physics, Berkeley (1966).
10. A. Browman, F. Liu, and C. Schaerf, Phys. Rev. 139, B1079 (1965).
11. S. D. Drell and J. D. Sullivan, Physics Letters 19, 516 (1966).
12. R. L. Anderson, D. Lundquist, and D. Ritson, Verbal report to XIII International Conference on High Energy Physics, Berkeley (1966).
13. J. C. Bizot, J. M. Buon, J. Lefrancois, J. Perez y Jorba, and Ph. Roy, Orsay Report (LAL 1138) June 1965.
14. L. H. Chan, K. W. Chen, J. R. Dunning, N. F. Ramsey, J. K. Walker, and Richard Wilson, Phys. Rev. 141, 1298 (1966); and F. M. Pipkin, Proceedings of the International Conference on Elementary Particles, Oxford (1965).
15. T. Massam and A. Zichichi, Proceedings of the International Conference on Elementary Particles, Oxford (1965); and submitted to XIII International Conference on High Energy Physics, Berkeley (1966).
16. Shin Ishida, Kimiaki Konno, and Hajime Shimodaira, submitted to XIII International Conference on High Energy Physics, Berkeley (1966).
17. G. Cocho, C. Fronsdal, Harun Ar-Radshid, and R. White, Phys. Rev. Letters 17, 275 (1966).
18. S. Coleman, Remarks to XIII International Conference on High Energy Physics, Berkeley (1966). G. Feldman and P. T. Matthews (Imperial College Preprint) and Remarks to XIII International Conference on High Energy Physics, Berkeley (1966).
19. H. Leutwyler, Phys. Rev. Letters 17, 156 (1966).
20. W. C. Barber, B. Gittelman, G. K. O'Neill, and B. Richter, Phys. Rev. Letters 16, 1127 (1966). In addition to ρ^0 exchange ϕ and ω exchange can also be included in $G(q^2)$ with no significant effect.

21. T. T. Wu and C. N. Yang, Phys. Rev. 137, B708 (1965).
22. J. Friedman, G. Hartmann, and H. Kendall, submitted to XIII International Conference on High Energy Physics, Berkeley (1966); and private communication.
23. S. D. Drell, A. C. Finn, and Michael H. Goldhaber, submitted to XIII International Conference on High Energy Physics, Berkeley (1966).
24. A. Martin, Nuovo Cimento 37, 671 (1965). A. M. Jaffe, Phys. Rev. Letters 17, 661 (1966).
25. If the form of Eq. (10) is continued to time-like values of q^2 in accord with the analyticity properties of dispersion theory, there will be exponential growth of G unless $p \leq 1$ or $p/p+1 \leq 1/2$ in this case. This is not however a proof that polynomial boundedness requires us to limit $p \leq 1$ since Eq. (10) gives only the asymptotically leading term for large space-like values of q .
26. B. Barish, D. Fong, R. Gomez, D. Hartill, J. Pine, A. V. Tollestrup, A. Maschke, and T. F. Zipf, submitted to XIII International Conference on High Energy Physics, Berkeley (1966).
M. Conversi, T. Massam, T. H. Muller, A. Zichichi, Nuovo Cimento 40, 690 (1965).
27. E. Titchmarsh, "The Theory of Functions" (Oxford Press, 1939).
A. A. Logunov, Nguyen Van Hieu, and I. T. Todorov, Annals of Physics 31, 203 (1965).
28. R. Budnitz, L. Carroll, J. Chen, J. R. Dunning, M. Goitein, K. Hanson, C. Mistretta, J. K. Walker, and Richard Wilson, submitted to XIII International Conference on High Energy Physics, Berkeley (1966).

29. See however, V. E. Krohn and G. R. Ringo, *Phys. Letters* 18, 297 (1965).
30. C. W. Akerlof, W. W. Ash, K. Berkelman, C. A. Lichtenstein, A. Ramanauskas, and R. H. Siemann, submitted to XIII International Conference on High Energy Physics, Berkeley (1966).
C. W. Akerlof, W. W. Ash, K. Berkelman, and C. A. Lichtenstein, *Phys. Rev. Letters* 16, 147 (1966).
31. J. Allen, G. Ekspong, P. Sällström, and K. Fischer, *Nuovo Cimento* 32, 1144 (1964). D. Cassel, M. Barton, R. Crittendon, V. Fitch, and L. Leipuner (unpublished). M. M. Sternheim and R. Hofstadter, *Nuovo Cimento* 38, 1854 (1965). M. E. Nordberg and K. F. Kinsey, *Physics Letters* 20, 692 (1966).
32. J. D. Bjorken, S. D. Drell, S. C. Frautschi, *Phys. Rev.* 112, 1409 (1958).
33. S. D. Drell, International Symposium on Electron and Photon Interactions at High Energies, Hamburg (1965) (Springer Tracts in Modern Physics, Vol. 39).
There is also no interference term if the pairs are observed with asymmetric kinematics but without distinguishing the signs of the charges.
34. R. B. Blumenthal, D. C. Ehn, W. L. Faissler, P. M. Joseph, L. J. Lanzerotti, F. M. Pipkin, and D. G. Stairs, *Phys. Rev.* 144, 1199 (1966). F. M. Pipkin, report to XIII International Conference on High Energy Physics, Berkeley (1966).
35. E. Eisenhandler, J. Feigenbaum, N. B. Mistry, P. J. Mostek, D. R. Rust, A. Silverman, C. K. Sinclair, and R. M. Talman, *Bull. Am. Phys. Soc., Ser. II*, Vol. 11, No. 1, p. 20 (1966); and
— R. M. Talman, report to XIII International Conference on High Energy Physics, Berkeley (1966).

36. J. Asbury, W. K. Bertram, U. Becker, P. Joos, M. Rhode, A. J. S. Smith, S. Friedlander, C. Jordan, and C. C. Ting, Report by C. C. Ting to XIII International Conference on High Energy Physics, Berkeley (1966).
37. J. K. dePagter, A. M. Boyarski, G. Glass, J. I. Friedman, H. W. Kendall, M. Gettner, J. F. Larrabee, and Roy Weinstein, Phys. Rev. Letters 12, 739 (1964). J. K. dePagter, J. I. Friedman, G. Glass, R. C. Chase, M. Gettner, E. von Goeler, Roy Weinstein, and A. M. Boyarski, Phys. Rev. Letters 16, 35 (1966); and Report by Roy Weinstein to XIII International Conference on High Energy Physics, Berkeley (1966).
38. Moreover, an approximate theoretical analysis of the virtual Compton contributions has been made for the parameters of this experiment as well as for the e^+e^- pair experiments, and it was found that they are no larger than at most 2% of the Bethe-Heitler terms for total pair masses ≤ 600 MeV. See Refs. (33) and (32).
39. F. J. M. Farley, J. Bailey, R. C. A. Brown, M. Giesch, H. Jöstlein, S. van der Meer, E. Picasso, and M. Tannenbaum, report to XIII International Conference on High Energy Physics, Berkeley (1966).
40. G. Charpak, F. J. M. Farley, R. L. Garwin, T. Müller, J. C. Sens, and A. Zichichi, Nuovo Cimento 37, 1241 (1965).
41. A. Petermann, Helv. Phys. Acta 30, 407 (1957). C. M. Sommerfield, Phys. Rev. 105, 1931 (1957). H. H. Elend, Physics Letters 21, 720 (1966). N. Kroll (unpublished).
42. E. R. Cohen and J. W. M. DuMond, Rev. Mod. Phys. 37, 537 (1965).
43. L. W. Durand III, Phys. Rev. 128, 441 (1962).

44. G. Segre', Physics Letters 7, 357 (1963).
45. It also contributes to the photon vacuum polarization. M. A. B. Beg, Phys. Rev. 134, B1368 (1964).
46. S. D. Drell and J. S. Trefil (unpublished).
47. S. B. Crampton, D. Kleppner, and N. F. Ramsey, Phys. Rev. Letters 11, 338 (1963).
48. For a general review and reference to all earlier work, see S. J. Brodsky and G. W. Erickson, Annals of Physics (in press).
49. E. S. Dayhoff, S. Triebwasser, and W. E. Lamb Jr., Phys. Rev. 89, 106 (1953).
50. C. K. Iddings, Phys. Rev. 138, B446 (1965).
51. The theoretical expression involves an integration over the electromagnetic form factors for all space-like momentum transfers. Since this requires an extrapolation beyond the experimental data at hand there is a numerical uncertainty. The result given in Eq. (18) is based on a series of different extrapolations that fit the available data and decrease smoothly to 0 as $q^2 \rightarrow \infty$. See Ref. (50).
52. R. T. Robiscoe, Phys. Rev. 138, A22 (1965). R. T. Robiscoe and B. L. Cosens, Phys. Rev. Letters 17, 69 (1966).
53. A. Verganelakis and D. Zwanziger, Nuovo Cimento 39, 613 (1965).
54. S. D. Drell and J. D. Sullivan, Report to XIII International Conference on High Energy Physics, Berkeley (1966); and Phys. Rev., to be published.
55. F. Guérin has also just completed a more detailed analysis of the contributions of non-resonant channels to the hfs without finding any sizable contributions (private communication from Orsay).

56. W. Cottingham, *Annals of Physics* 25, 424 (1963).
A. C. Finn (unpublished).
57. R. Dashen and S. Frantschi, *Phys. Rev.* 135, B1190 (1964).
R. Dashen, *Phys. Rev.* 135, B1196 (1964).
H. Pagels, *Phys. Rev.* 144, 1261 (1966).
H. Fried and T. Truong, *Phys. Rev. Letters* 16, 559 (1966).
G. Shaw and D. Wong, *Phys. Rev.* (to be published).
58. A. Bohr, *Phys. Rev.* 73, 1109 (1948).
F. Low, *Phys. Rev.* 77, 361 (1950).
59. W. E. Cleland, J. M. Bailey, M. Eckhause, V. W. Hughes, R. M. Mobley, R. Prepost and J. E. Rothberg, *Phys. Rev. Letters* 13, 202 (1964).
60. M. A. Ruderman, Report to XIII International Conference on High Energy Physics, Berkeley (1966).
61. M. Soto (to be published).
62. G. W. Erickson and D. R. Yennie, *Annals of Physics* 35, 271 (1965).
63. A new approach to Lamb shift calculations based on dispersion theory was reported to the XIII International Conference on High Energy Physics, Berkeley (1966) by R. Omnés.
X. Artru, J. L. Basdevant, and R. Omnés (to be published).
64. N. Kroll, Contribution to XIII International Conference on High Energy Physics, Berkeley (1966); and *Phys. Rev.* (in press).
65. J. A. McClure and S. D. Drell, *Nuovo Cimento* 37, 1638 (1965).

FIGURE CAPTIONS

- Fig. 1 - Test of the Rosenbluth straight line for $q^2 = 1.5 \text{ (GeV/c)}^2$.
- Fig. 2 - New values for the proton form factors presented to the conference by groups working at DESY. Points without error flags have errors less than the size of the symbol. Cross marks on the error flags indicate the uncertainty in (G_M/μ) if $G_E = G_M/\mu$ is assumed.
- Fig. 3 - Interference between two-photon and one-photon exchange amplitudes leading to a difference between positron-proton and electron-proton scattering.
- Fig. 4 - Collection of data on $R = \sigma(e^+p)/\sigma(e^-p)$.
- Fig. 5 - Diagram for neutral vector meson contributions to the proton form factors.
- Fig. 6 - Comparison of the dipole and the SL (6,C) predictions with the proton form factors using the new DESY results (note the scale change between the two graphs). An average was taken at momentum transfers having more than one determination of the form factors. The errors of points without error flags are less than the size of the symbol. The values of G_M above $\sim 4 \text{ (GeV/c)}^2$ were obtained using the assumption $G_E = G_M/\mu$.
- Fig. 7 - Comparison with data of the Wu-Yang proton form factor prediction for large q .

Fig. 8 - Values of the square of the deuteron form factor. For the angles and energies of these experiments the scattering is predominantly charge scattering. In reducing the observed cross sections to $|F_D|^2$ the nucleon isoscalar charge form factor has also been divided out.

Fig. 9 - Comparison of a fractional exponential form factor and of a theoretical form based on a potential model with a $1/r^4$ repulsive core with the new proton form factor data for large q .

Fig. 10 - Comparison of the upper limit for the proton form factor in the time-like region with the dipole distribution which has been found to fit the scattering data well in the space-like region. Also indicated are the positions of the ρ^0 , ω , and ϕ resonances.

Fig. 11 - Comparison of new data on the electron-neutron cross sections with the indicated scaling laws for the nucleon form factors.

Fig. 12 - Diagram for the one pion exchange contribution to the electropion production amplitude. At the pole of the intermediate exchanged pion the blob at (A) is just the pion charge form factor $F_\pi(q^2)$.

Fig. 13 - Diagrams for Bethe-Heitler and virtual Compton contributions to the wide angle pair production cross sections. The lepton pairs are formed in even and odd charge conjugation states, respectively, as indicated.

Fig. 14 - Comparison of wide angle electron-positron pair production experiments with theory as a function of the total pair mass. The Cornell points include radiative corrections and the CEA-Harvard results are shown normalized with the new radiative corrections. The DESY-Columbia data is preliminary and has not yet been completely adjusted for radiative corrections (an additional $\sim 5\%$ and constant).

Fig. 15 - Comparison of wide angle muon pair production data with theory as a function of the momentum transfer to the virtual muon line. The ascending slope at the largest momentum values is due to ρ^0 formation followed by the decay $\rho^0 \rightarrow \mu^+ + \mu^-$.

Fig. 16 - Initial CERN data on μ^- spin precession in the magnetic field of the muon storage ring.

Fig. 17 - Graph of a contribution to the muon $g - 2$ value coming from vacuum polarization correction to the photon propagator.

Fig. 18 - Graph of a contribution to the muon $g - 2$ value of first order in the weak coupling strength if the W meson exists.

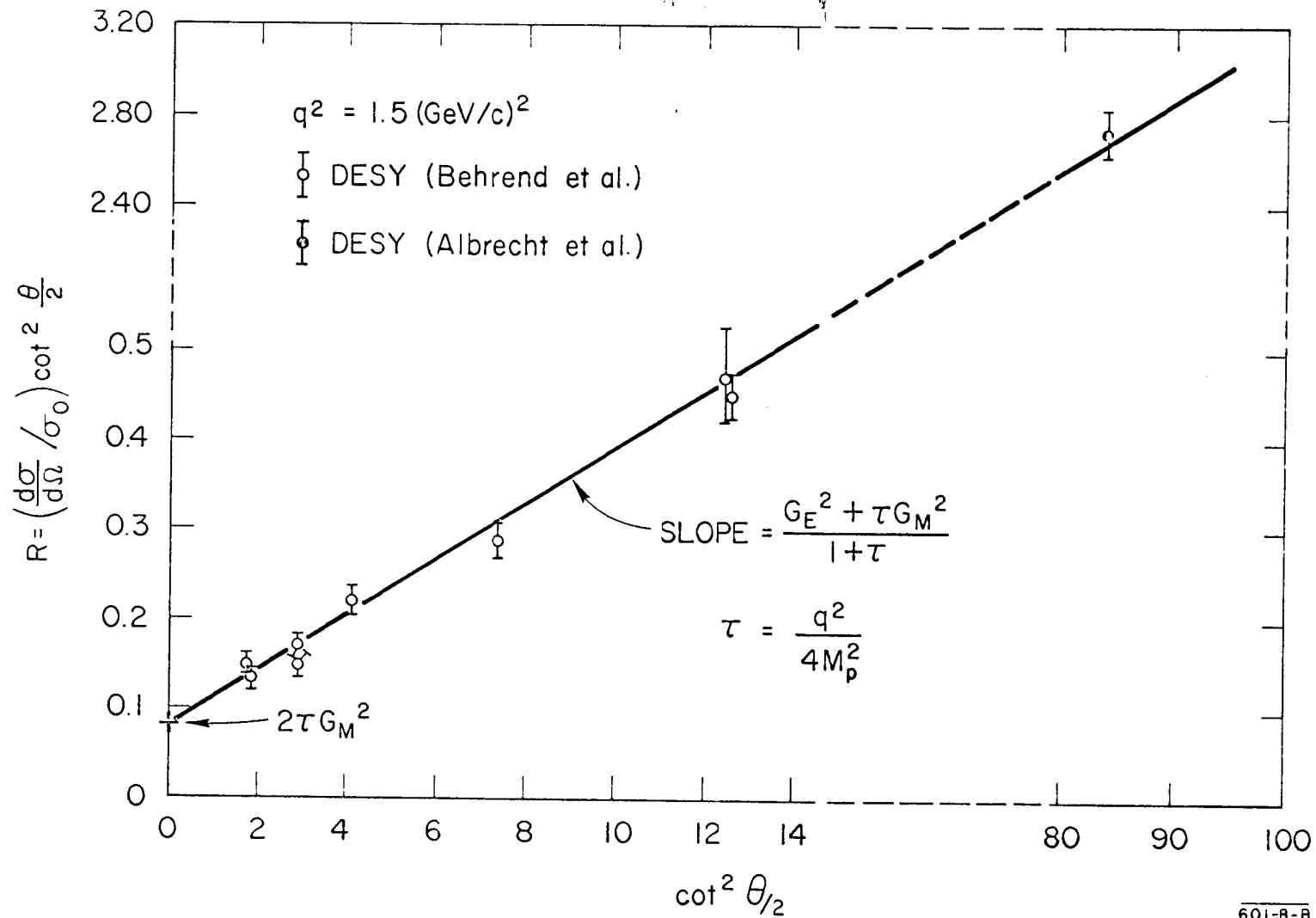


FIG. 1

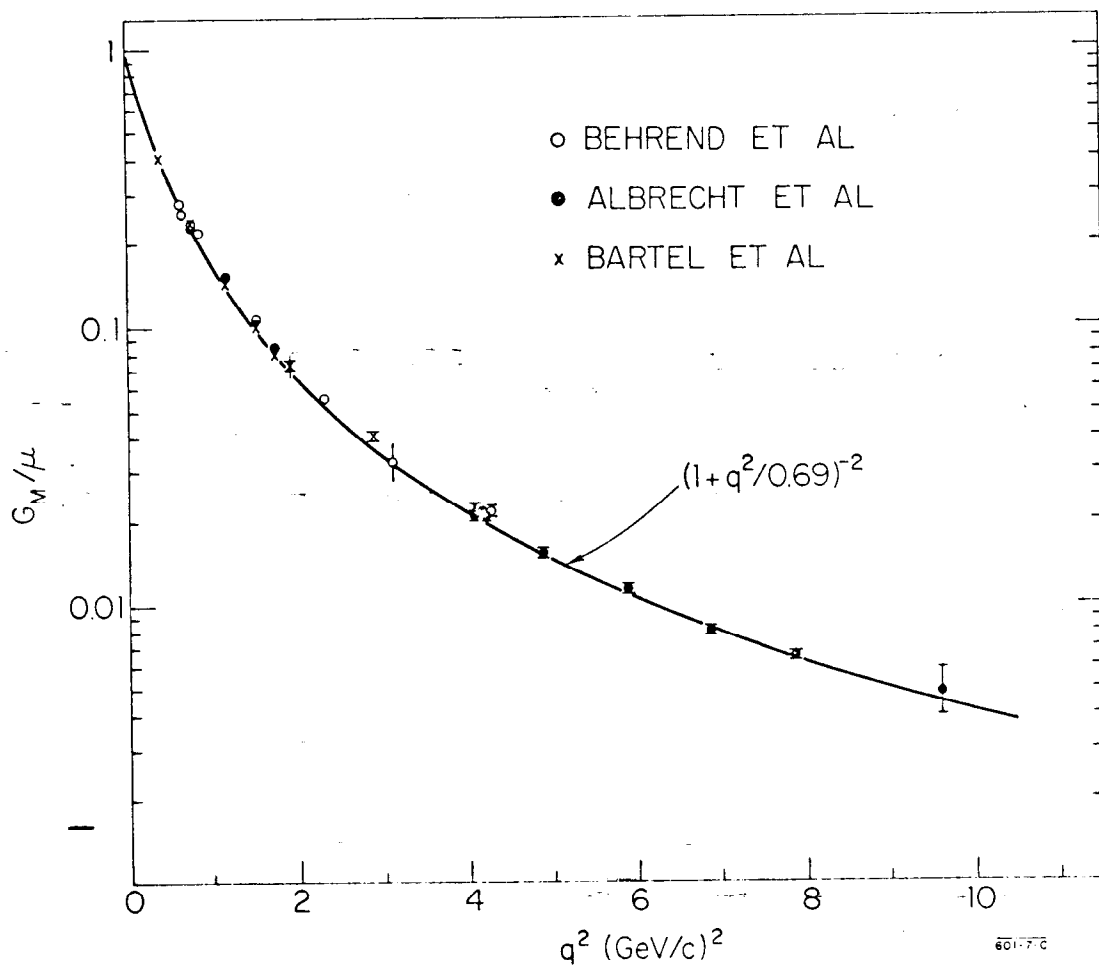
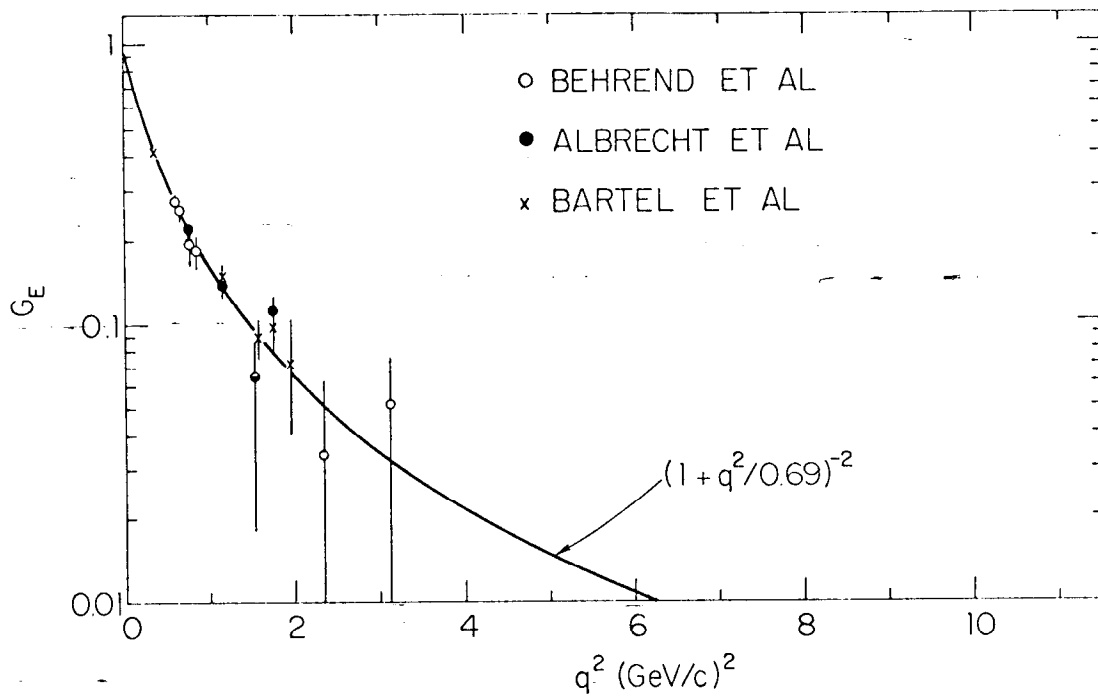
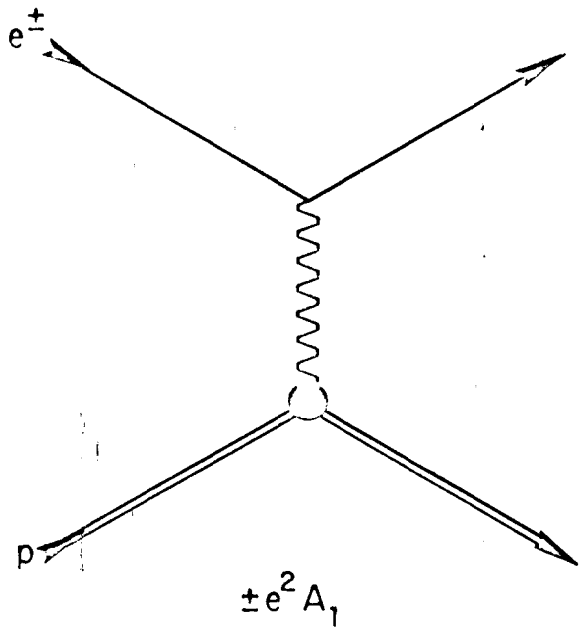
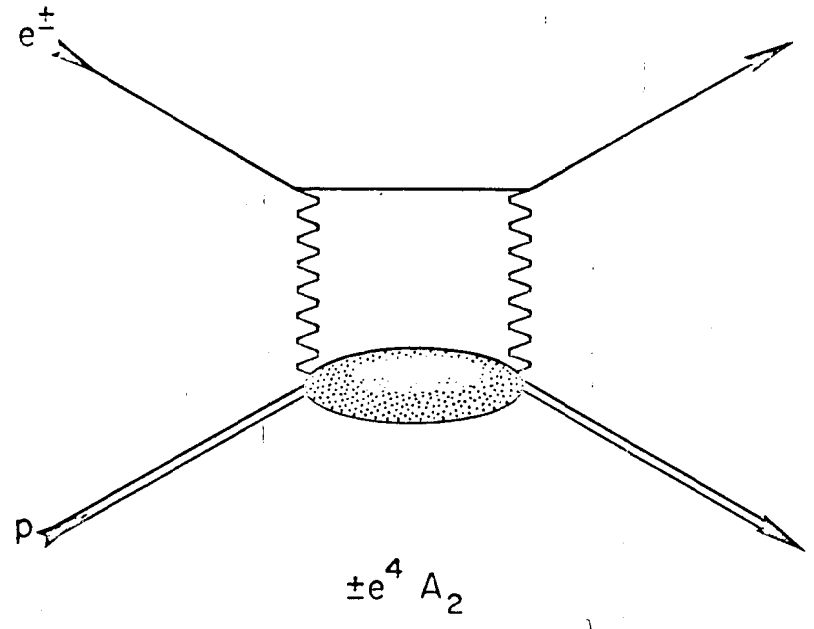


FIG. 2



+

+



$$R = \frac{\sigma(e^+p)}{\sigma(e^-p)} \cong 1 + 4e^2 \frac{\text{Re}(A_1 A_2^*)}{|A_1|^2}$$

601-6-A

FIG. 3

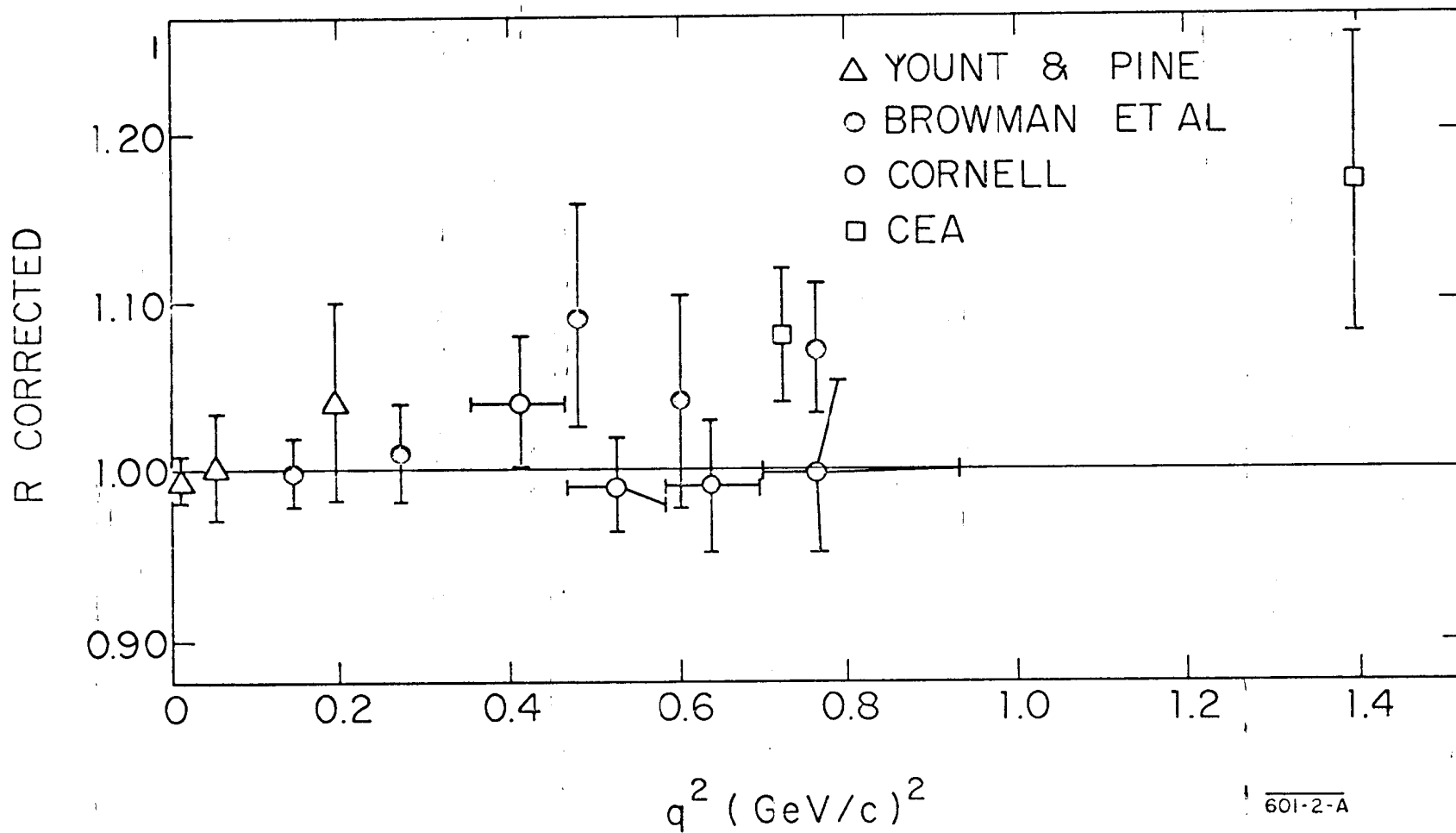


FIG. 4

601-2-A

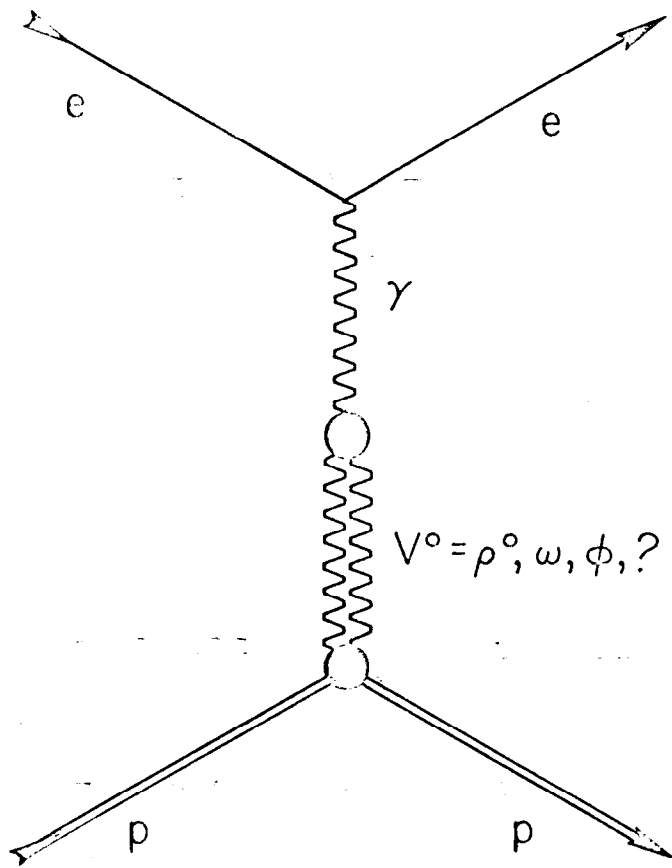
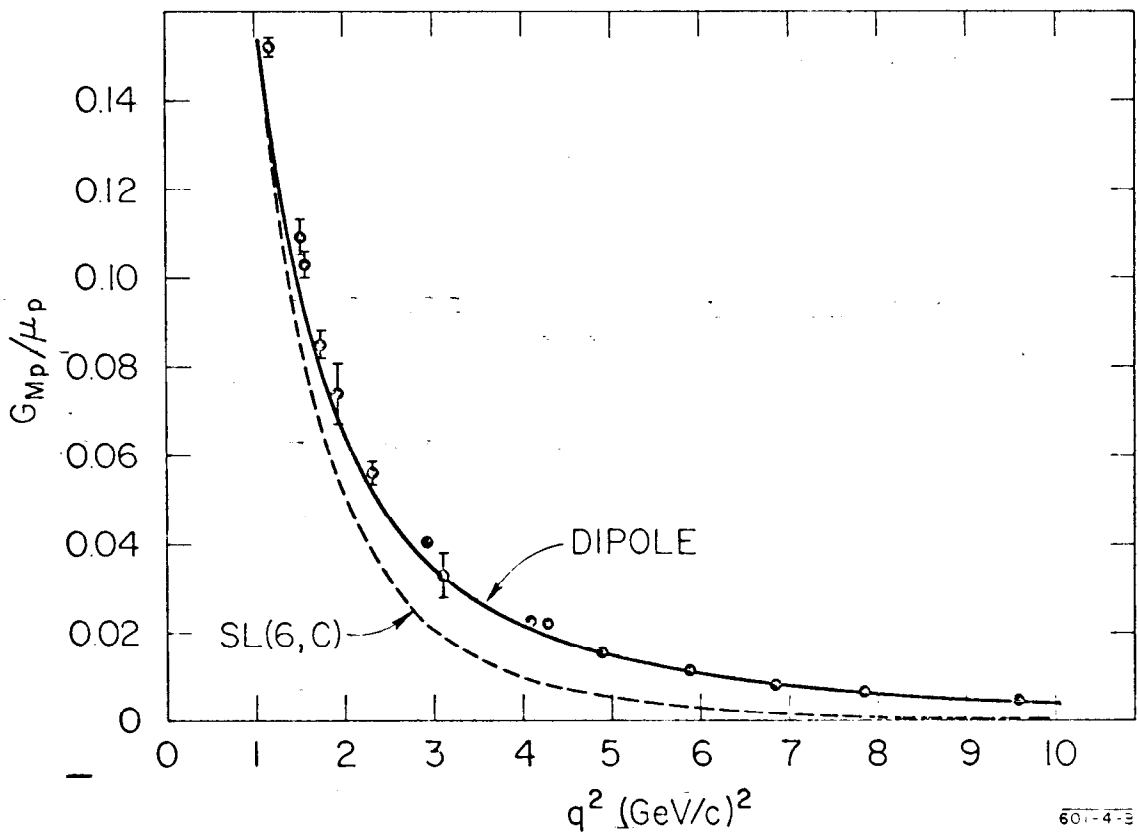
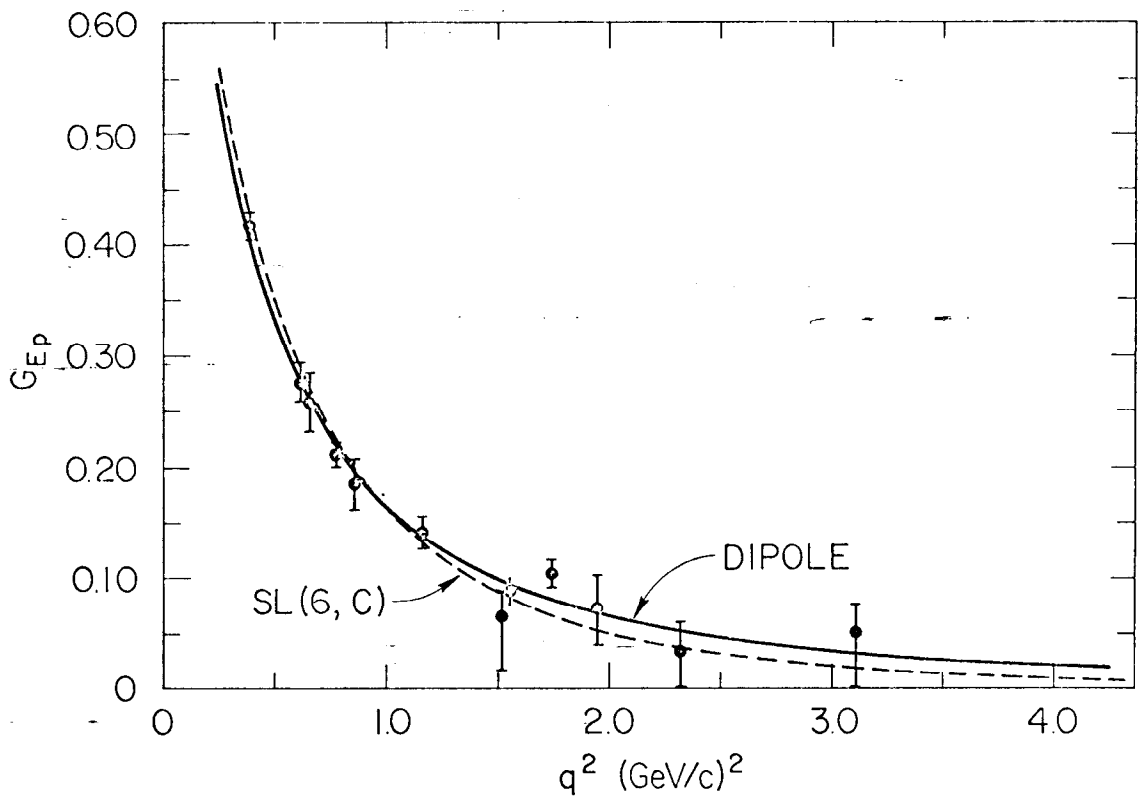


FIG. 5

601-5-A



60-4-3

FIG 6

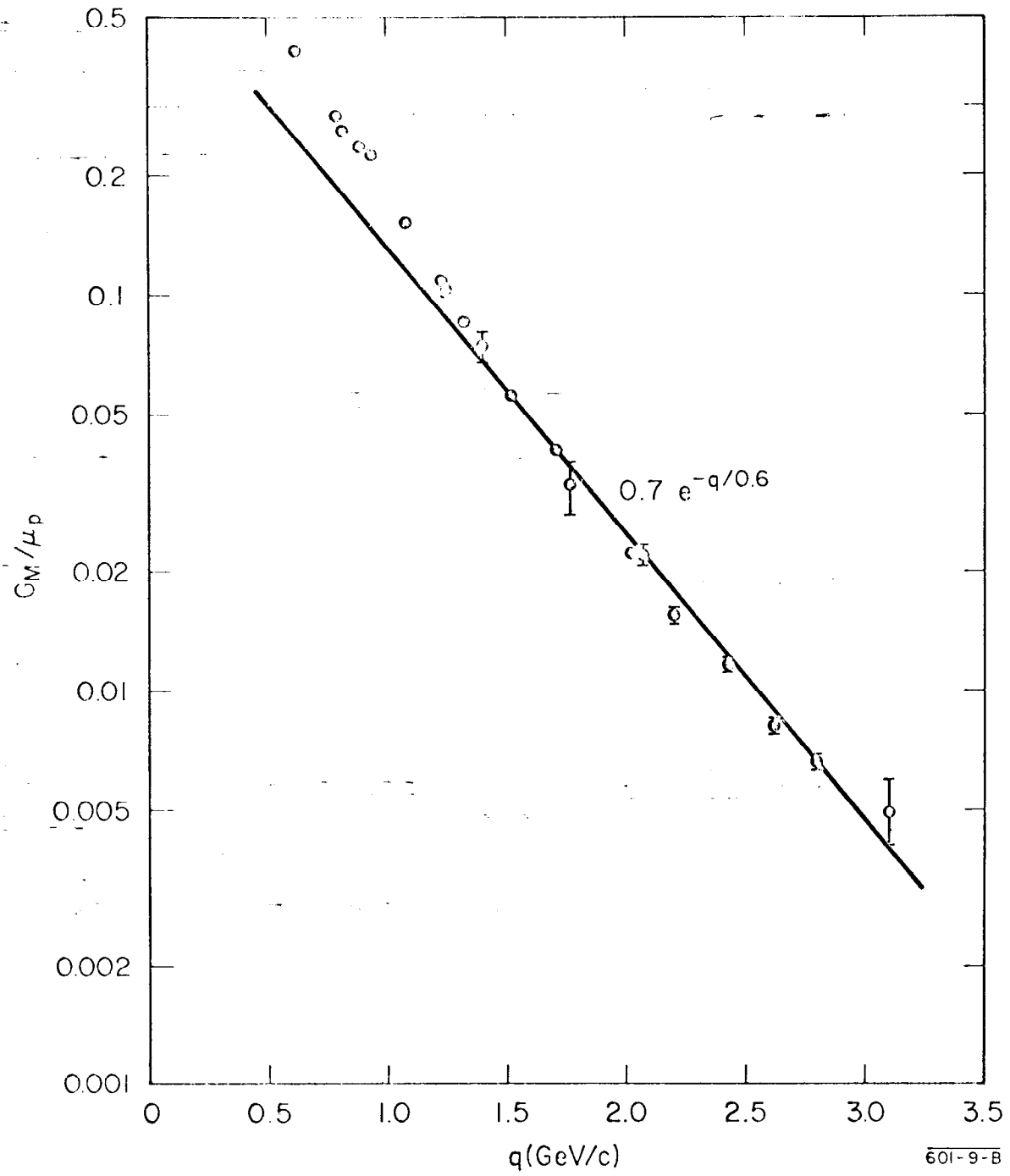


FIG. 7

601-9-B

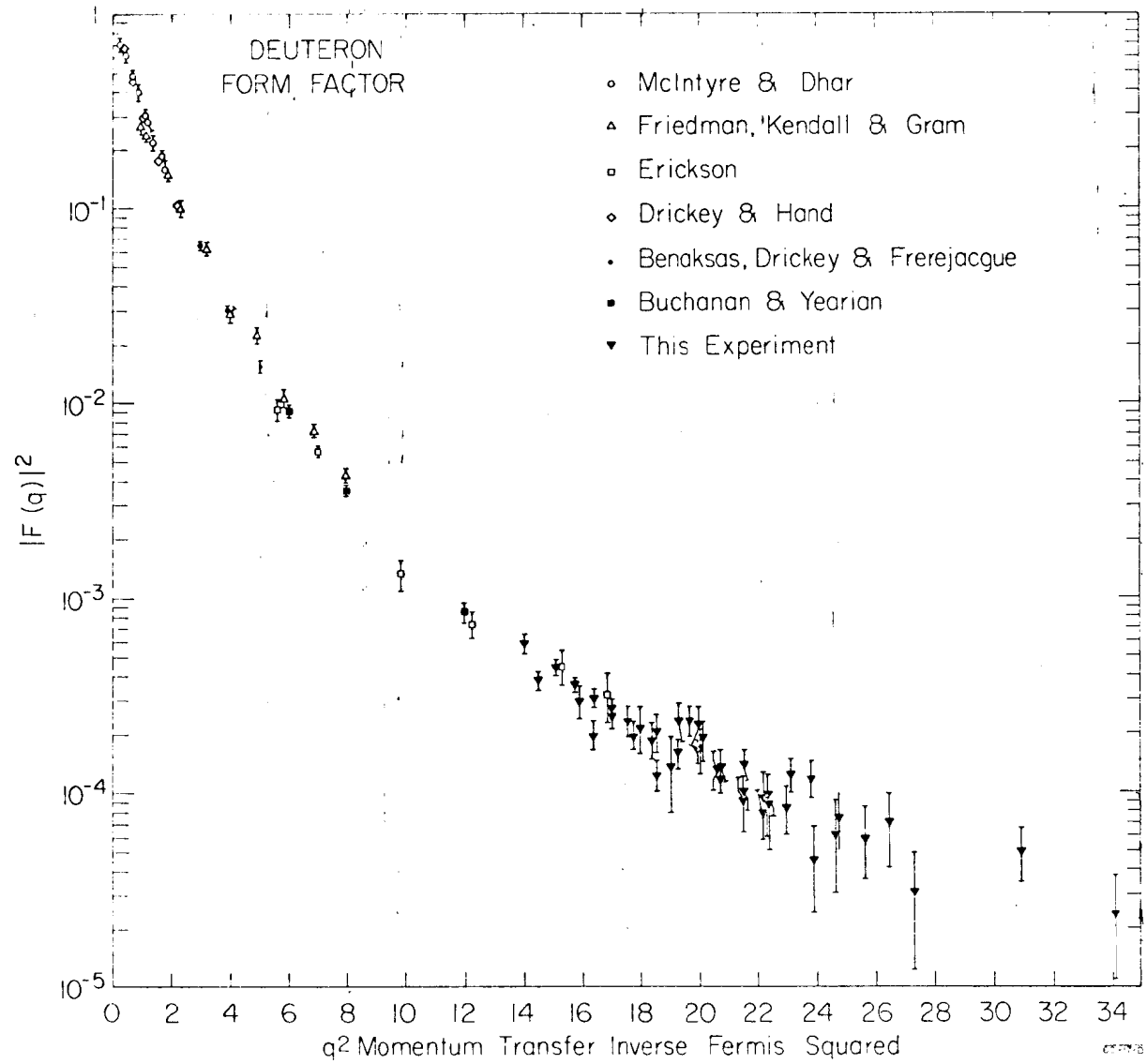


FIG 8

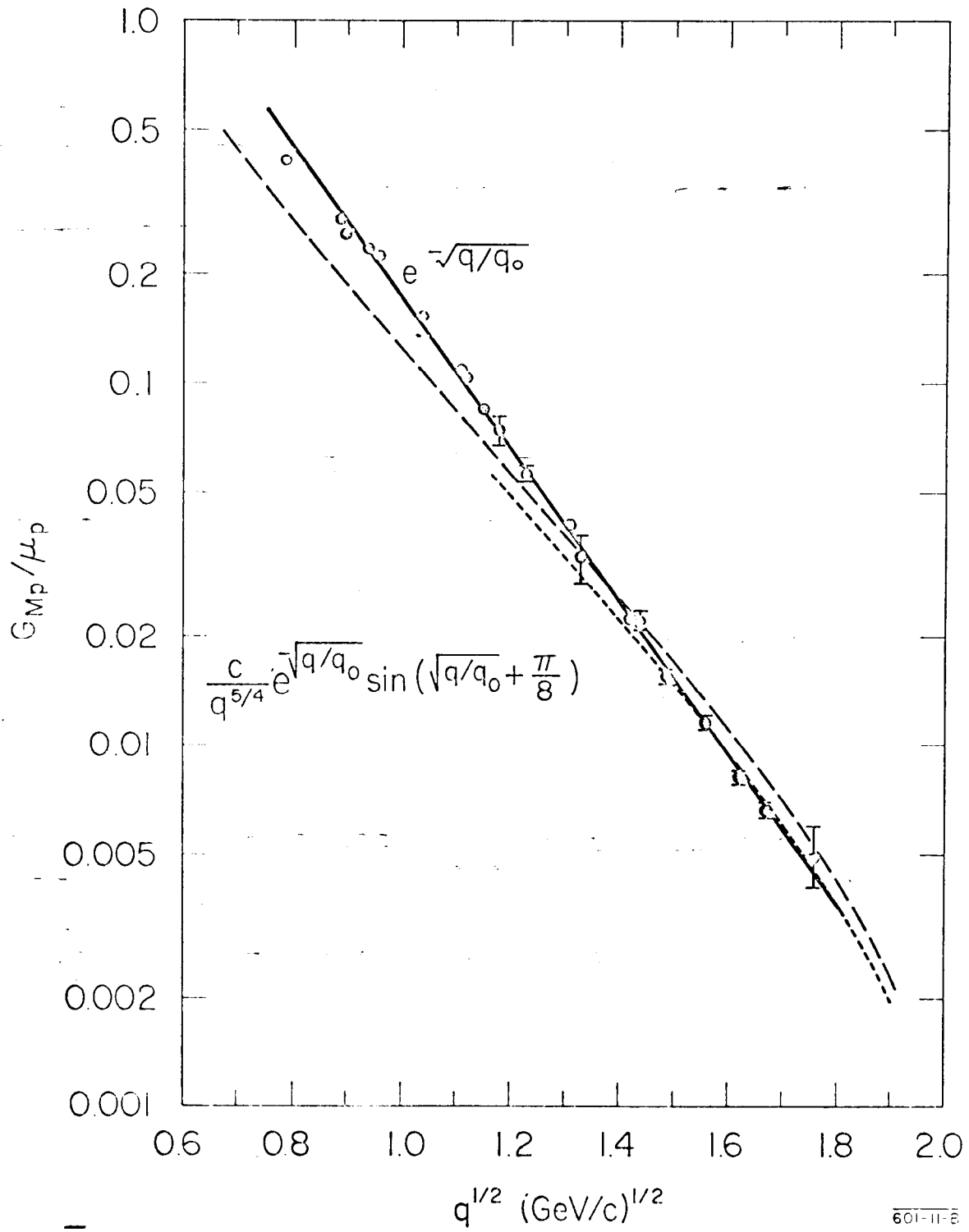


FIG. 9

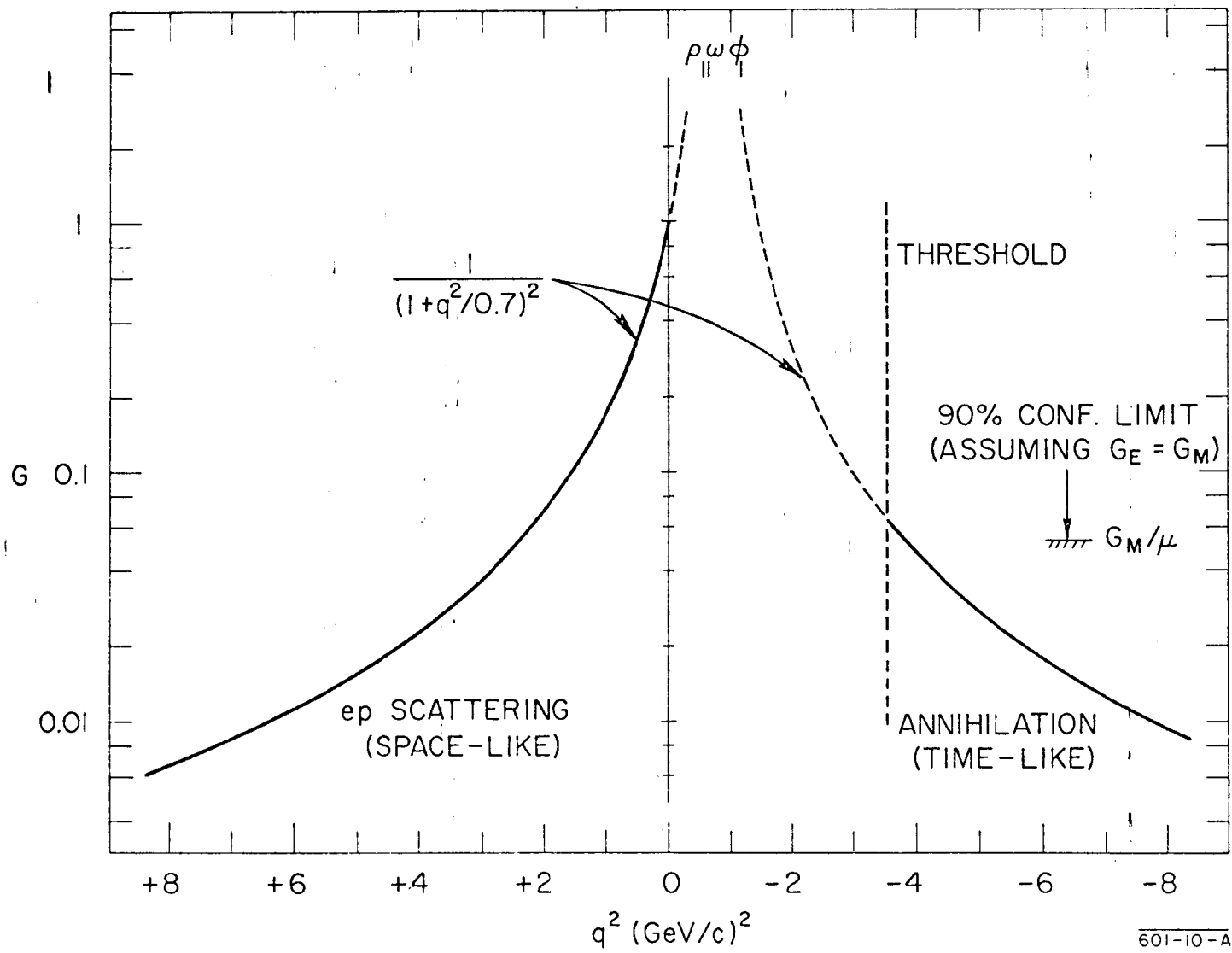
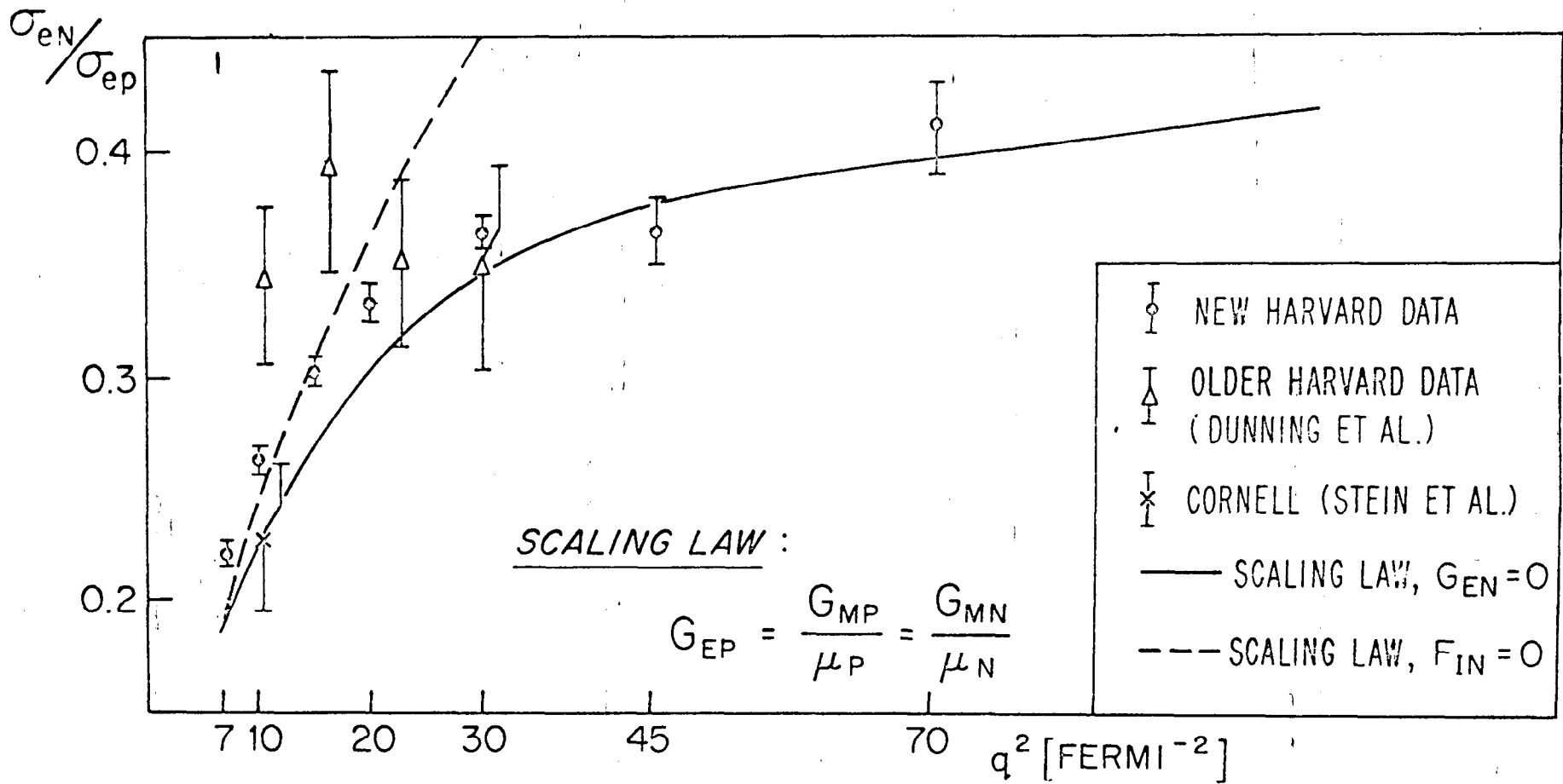
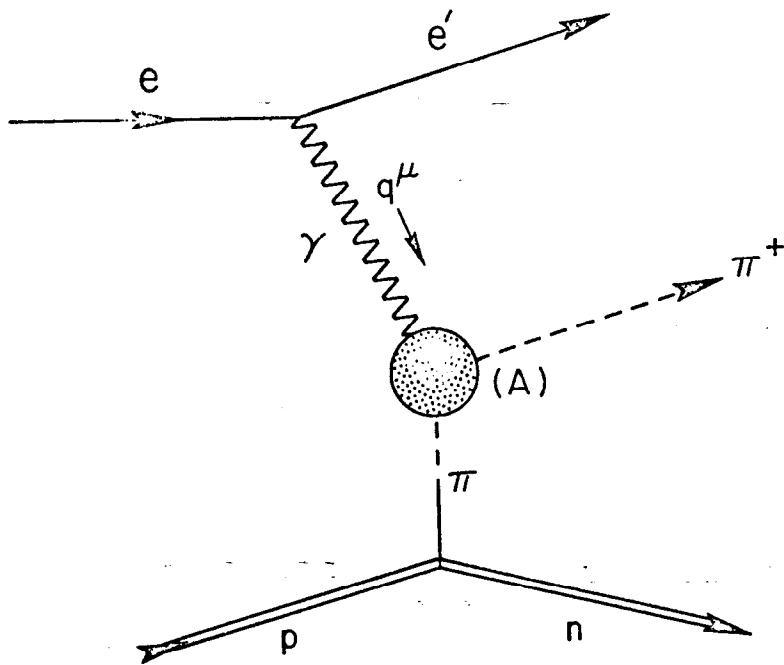


FIG. 10



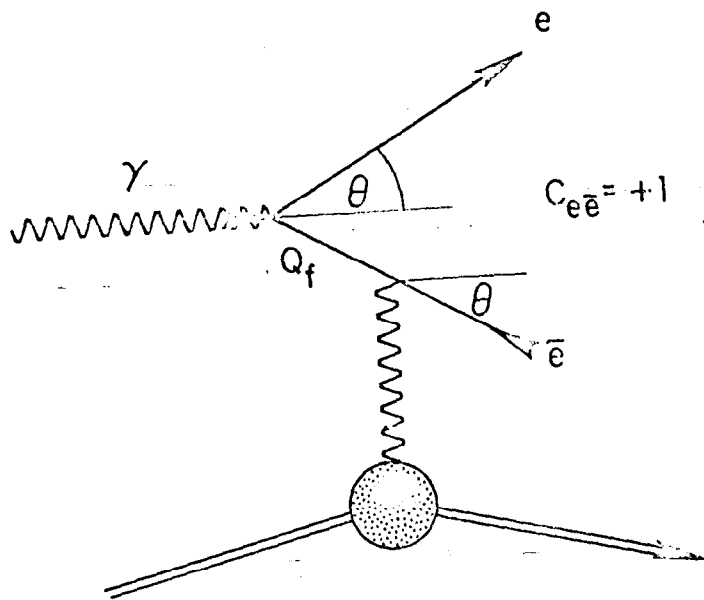
RATIO OF NEUTRON TO PROTON CROSS-SECTIONS AT 20°

FIG 11



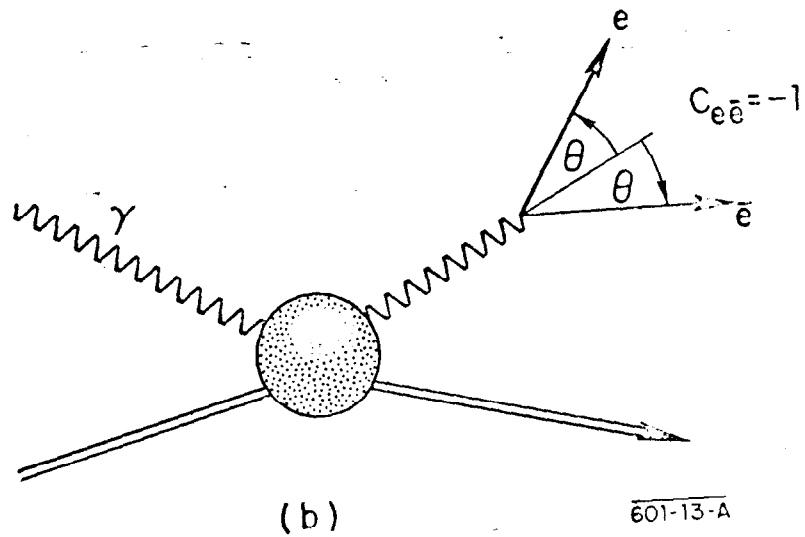
601-12-A

FIG. 12



$$\begin{aligned}
 2Q_f^2 &= (\text{invariant mass})^2 = Q_M^2 \\
 &= (p + \bar{p})^2
 \end{aligned}$$

(a)



601-13-A

FIG. 13

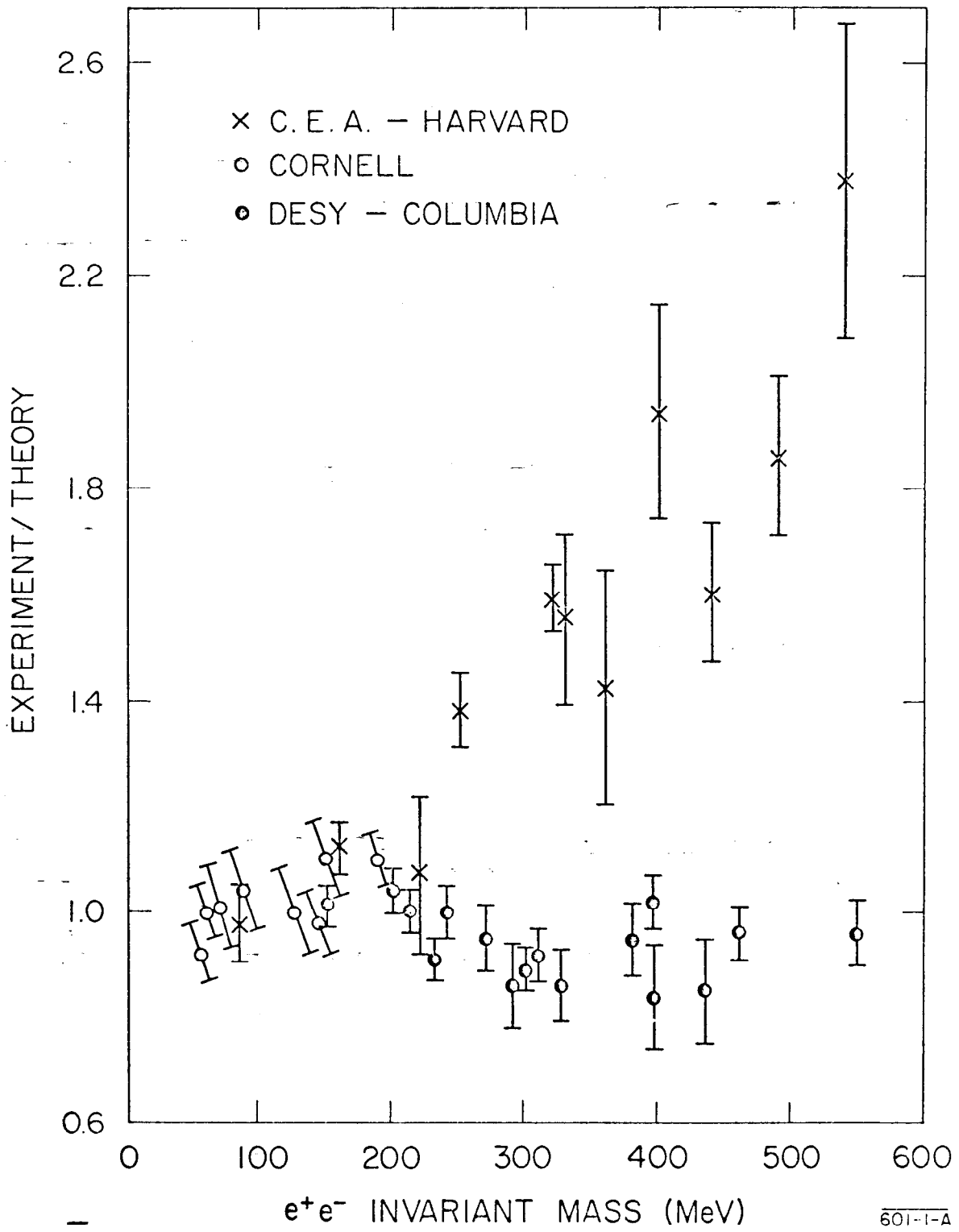


FIG. 14

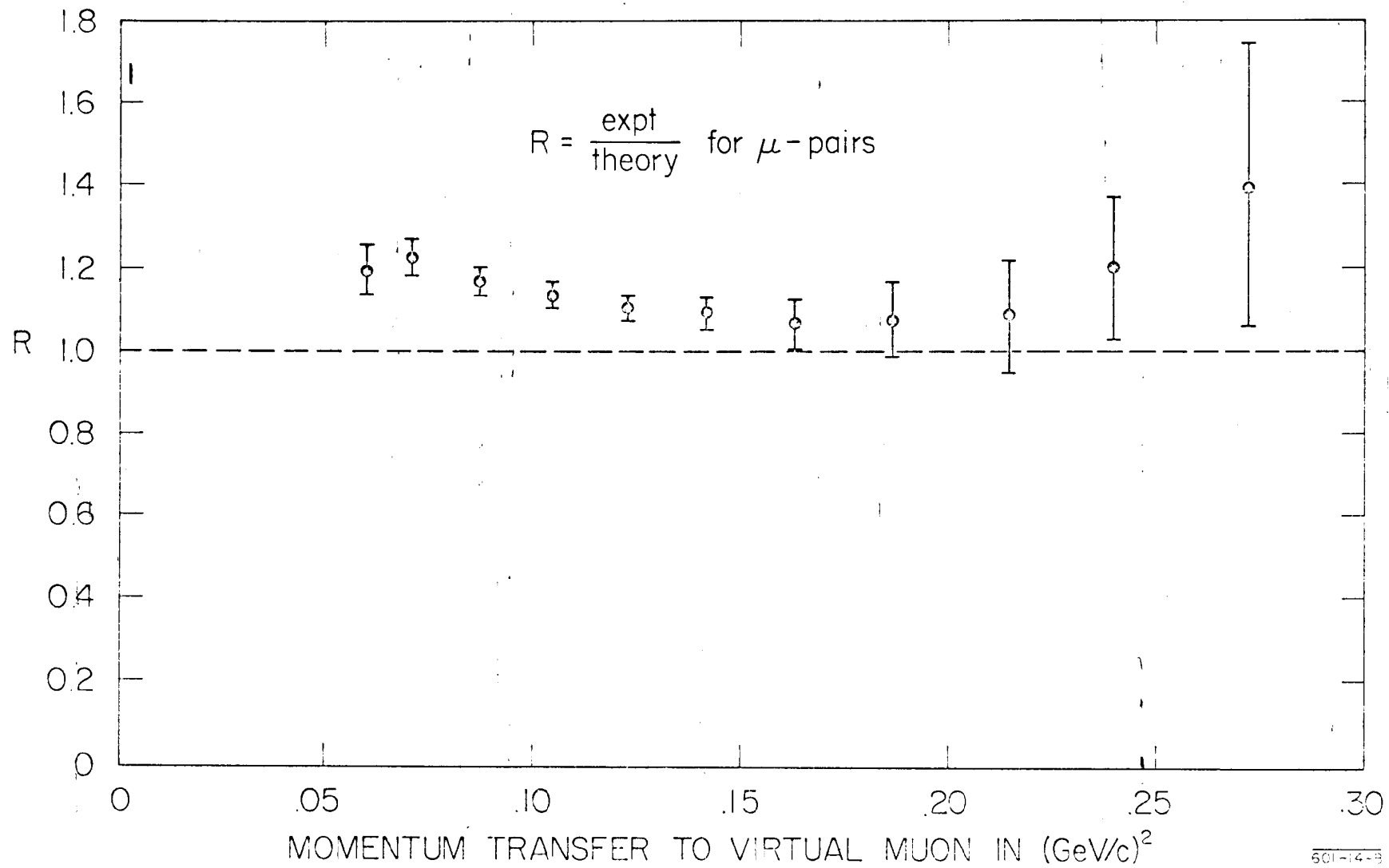


FIG. 15

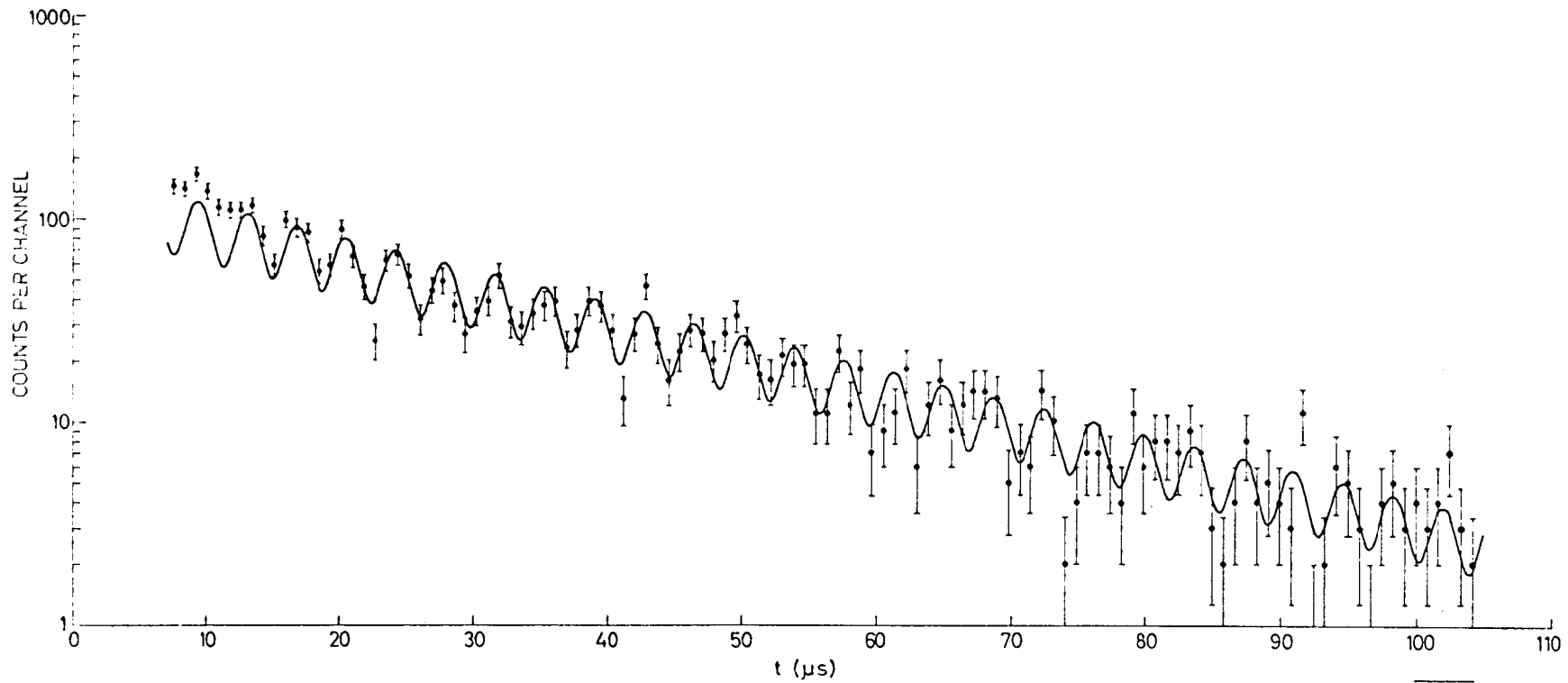


FIG. 16

601-3-A

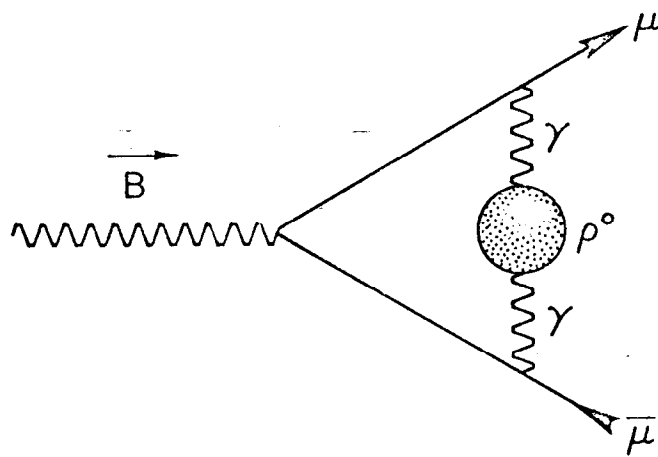


FIG. 17

601-15-A

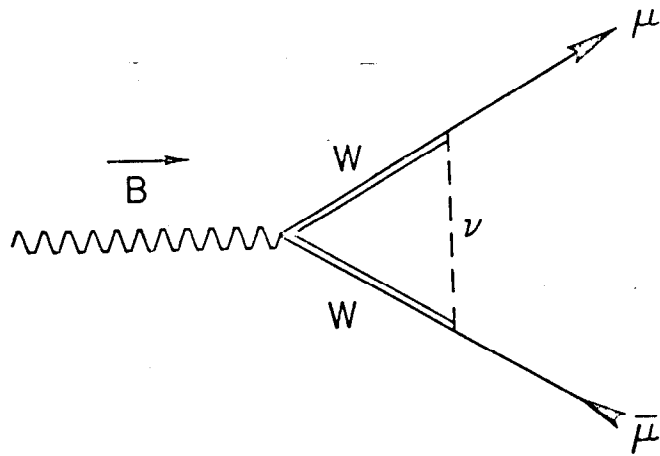


FIG. 18

601-16-A